2016

An investigation of cell responses to mechanical environment

Jia Hu
Lehigh University

An Investigation of Cell Responses to Mechanical Environment

by

Jia Hu

Presented to the Graduate and Research Committee

of Lehigh University

in Candidacy for the Degree of

Doctor of Philosophy

In

Mechanical Engineering

Lehigh University

May 2016

Approved and recommended for acceptance as a dissertation in partial fulfillment of the requirements for the degree of Doctor of Philosophy.

_____

Date

_____

Dr. Yaling Liu, Dissertation Advisor

_____

Accepted Date

Committee Members:

_____

Dr. Daniel Ou-Yang

_____

Dr. Arkady Voloshin

_____

Dr. Xiaohui (Frank) Zhang

Acknowledgements

I would like to thank my advisor, Dr. Yaling Liu for the opportunity to develop this study and for his guidance during years of study. I would also like to express my gratitude to my committee members, Dr. Arkady Voloshin, Dr. Daniel Ou-Yang and Dr. Xiaohui Zhang for their excellent advice and experience. I am deeply indebted to my lab members of the Bionanomechanics group, Antony Thomas, Wentao Shi, Shunqiang Wang, Ran He, and Christopher Uhl for their kind help and advice. I would also like to thank the staffs in bioengineering department of Lehigh University; Susan Perry, Will Xia and Lee Graham for graciously providing research space and guidance of the experimental facilities in the bioengineering laboratory. I would also like to thank the journal, PLOS ONE and journal of nanomaterials, for granting permission to use my published work in this dissertation.

To my family and friends, a gracious thank you is well deserved. To my parents, I owe especial thanks for their encouragement, tremendous patience and great support to me throughout my years at Lehigh. Without their support, this would have not been possible.

Table of Contents

List of figures

Abbreviations

BOEC	Bovine aortic endothelial cell
PDMS	Polydimethylsiloxane
PGA	Polyglycolic acid
PLGA	Poly (lactic-co-glycolic acid)
SEM	Scanning electron microscope
NP	Nanoparticle
MPS	3-mercaptopropyltrimethoxysilane
DMF	Dimethylformamide
DEP	Dielectrophoresis
ROS	Reactive oxygen species
QD	Quantum dots
CSK	Cytoskeleton

Abstract

With the development of in vitro systems for tissue engineering, various substrates and mechanical stimuli have been utilized to modulate the cell behavior. It's known that various micropatterns have been fabricated and applied to regulate cell adhesion, morphology and function. Micropatterns created by standard photolithography process are usually rectangular channels with sharp corners (microgrooves) which provide limited control over cells and are not favorable for cell-cell interaction and communication. We propose a new micropattern with smooth wavy surfaces (micro-waves) to control the position and orientation of cells. Results showed that cells adhered to the wavy surface displayed both improved alignment and adhesion strength compared to those on the flat surface. Shear flow was further applied to examine the cell adhesion response to the flow.

In recent years, nanoparticles (NPs) have gained increasing interest due to its potential use as drug delivery, imaging and diagnostic agents in pharmaceutical and biomedical applications. While lots of cells *in vivo* are under mechanical forces, little is known about the correlation of the mechanical stimulation and the internalization of NPs into cells. We investigate the effects of applied cyclic strain on NPs uptake by bovine aortic endothelial cells (BAECs). The cyclic strain results in a significant enhancement in NP uptake which increases almost linearly with strain level.

In my study, micro-patterned substrates, shear flow and cyclic strain have been applied to investigate the cell behavior including cell alignment, cell spreading, cell adhesion and cellular uptake of NPs. Studies of cells response to these mechanical stress promote our current understanding of how cells sense and response to their mechanical environment.

Chapter 1 - Introduction

In recent decades, significant efforts have been made for development of tissue engineering *in vitro*. Some mammalian cell types are anchorage-dependent and will die if are not cultured on a cell-adhesion substrate. Biomaterials provide a cell-adhesion substrate and also control the structure and function of the cells in a predesigned manner. A range of factors affects the behavior of cells on the structured surfaces, including surface chemistry, feature geometry, feature aspect ratio and differences in the cell types used[1]. In my study, I investigated cell adhesion and alignment on substrate with different features. Meanwhile, it is well known that tissues and cells in the human body are exposed to a range of different external forces, which influence their development and maintenance. In the blood vessel, mechanical forces in the form of tension, compression, and fluid-induced shear are all present but the nature of these forces is not well understood, neither is what effect they have on endothelial cell (EC)behavior and function. In my research, ECs were exposed to fluid-induced shear and cyclic stress that mimic the *in vivo* condition. Investigations were conducted to further understand the mechanism and influence of such mechanical stimulation on ECs. Various mechanical stimuli such as shear flow and cyclic stretch have been investigated to modulate the cell responses, including cell alignment, adhesion, proliferation and cell-cell interaction. In our study, we examined the cell responses to shear flow and cyclic strain.

1.1 Substrate pattern modulate the cell alignment and adhesion

Cells are usually cultured on biocompatible substrates. The ideal biomaterials substrate should be biocompatible, promote cellular interaction, and possess proper mechanical and physical properties. Many classes of biomaterials have been used for cell-based tissue engineering, including naturally derived materials (e.g. collagen and alginate), and synthetic polymers (e.g. polyglycolic acid [PGA], poly (lactic-co-glycolic acid) [PLGA], polydimethylsiloxane [PDMS]). An advantage of synthetic polymers is reproducible large-scale production with controlled properties of strength, degradation rate, and microstructure. PDMS is the most widely used silicon-based organic polymer due to its biocompatibility, transparency, deformability, low cost and unusual rheological properties. Some proteins such as collagen and gelatin contain cell-adhesion domain sequences which exhibit specific cellular interactions. This may assist in retaining the phenotype and activity of many types of cells, including ECs and fibroblasts. A layer of protein can be coated on the PDMS substrate to enhance the cell adhesion and proliferation. PDMS has high elasticity so it's convenient to stretch the PDMS membrane with a stretcher. More importantly, it has a big benefit as the most widely used microfluidic channel fabrication material which can be used for drug delivery, shear flow testing and cell isolation and selection.

The PDMS membrane can be micro-patterned in order to confine cells or tissues to a specific geometry. Cells must adapt to the substrate geometry to form tissue integrity. A lot of nano/micro-patterns have been printed on the PDMS membrane with UV technique. Investigations were made to examine the cells patterning on these substrates.

Understanding the interaction between cells and a micro-patterned surface is important for tissue engineering, i.e., cell growth and cell-cell communication. Cell patterning technique, which provides the basis approach for manipulating cells, play an important role for understanding functions of both individual cells and cell-cell interaction[2, 3]. However, conventional methods such as photolithography, contact printing and ink-jet printing [4] cannot precisely control cell behaviors. Physical effects, especially topographic or mechanical effects can be applied for better control of cell patterning. The ability to control the position of cells in an organized pattern on a substrate has become increasingly important for the development of cellular biosensor technology and tissue engineering applications [5-7].

For individual cells, adhesion to the extracellular matrix or to the cell culture substratum when grown in vitro plays an essential role for many processes such as proliferation and differentiation. The manipulation of cell growth through topographical features on a substrate can have significant applications in tissue engineering. With knowledge of cell behavior in response to such features, we can fabricate various substrates to control cell proliferation in favor of desired application. With the advent of nanofabrication techniques, a number of researchers have studied the effects of nano-scale grooves on cell spreading, migration, morphology, signaling and orientation [8-10]. When seeded onto a nano-grooved surface, cells orient themselves following the orientation of initial protrusions from the cell [11, 12]. Another study using skeletal muscle cells observed that submicron grooved pattern inhibited cell proliferation, and enhanced its differentiation capabilities [13]. Although nanogrooves could help cell alignment, they

cannot provide a good control of cell location since the groove dimensions are small compared to the cell size. In order to better control the cell location, a micro-pattern with size similar to the cells is needed.

PDMS membranes with micro-patterns have been studied to regulate the cell spreading and alignment [14-16]. One study using human osteo-sarcoma (HOS) cells on PDMS surfaces shows that microgroove spacing and height can influence the cell spreading and adhesion [17]. Microgrooves with well-controlled ridges and spacing were fabricated by curing poly-di-methy-siloxane (PDMS) in silicon molds produced by photolithography [17]. Culturing HOS cells on microgrooves with different spacing from 5 μm to 120 μm shows that cells aligned well in the directions of microgrooves when the groove spacing was comparable to the spread cell size [17]. However, the cell orientations became more random as the ridge separation increases [17].When the groove spacing is less than the size of fully spread cell, the height of ridges dominates the cell orientation [17].

Generally, a groove pattern with sharp corners has been used. While these grooves provide strong constrain on cells that resist the cell-cell interaction. Recently, a reconfigurable micro topographical system customized for cell culture and imaging that consists of reversible wavy micro features on poly (dimethylsiloxane) (PDMS) has been constructed. This reversible topography was able to align, unaligned, and realign C2C12 myogenic cell line cells repeatedly on the same substrate within 24h intervals, and did not inhibit cell differentiation (Figure 1-1) [18]. PDMS substrates were also used in order to apply mechanical force on cells, including shear flow and cyclic stretch.

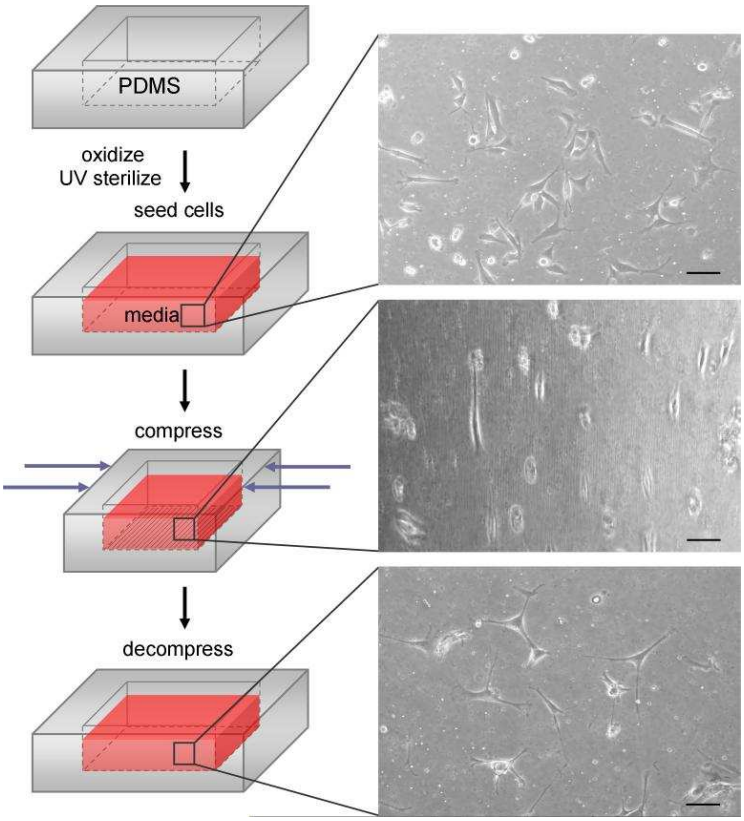

Figure 1- 1: Optical microscopy images of muscle cells on the reversible wavy surfaces; cell aligned along the waves and returned to random orientation on the uncompressed, flat surface within 24 h [1]. Scale bars = 50 μm.

1.2 Shear flow in microfluidic device regulates cell patterning

In the last two decades, thousands of researchers spent a huge amount of time to fabricate various microfluidic devices which can be applied for performing analytical and diagnostic assays. These microfluidic devices have many advantages including high sensitivity, low cost, short time testing, small laboratory space, well-fined laminar flow and controllable diffusion speed and size. Microfluidic devices have many applications such as cell isolation, nucleic acids extraction, drug screening, protein crystallization and chemical synthesis. PDMS with patterns are widely used as a component to assemble into microfluidic devices. As we know, microfluidic chip is a set of micro-channels etched or molded from some materials including glass, silicon or polymer such as PDMS. The micro-channels inside the microfluidic chip are connected together in order to achieve desired functions such as cell sorting, cancer cell capture, and fluid pump. The liquids are flowed into the micro-channels in the microfluidic chip through inputs to outputs. The use of diverse materials for the fabrication of microfluidics chip was based on photolithography technique, derived from the well-developed semiconductor industry. Nowadays, PDMS and soft-lithography are commonly used due to their easiness, low cost, well established and fast process. Researchers can rapidly build prototypes and test their functions in a controllable manner.

Blood vessels are constantly exposed to shear stress due to the blood flow in the vessel. The micro/nanopattern and the direction of shear stress were applied to mimic the *in vivo* environment with *in vitro* model. Biomimetic structures have been extensively studied due to its fine controllability for cellular microenvironments. The microfluidic based

artificial blood vessel system has been widely investigated due to its ability to produce vascular architectural similarity. It has been reported that the application of shear stress can provide guidance to the cell migration and elongation in the *in vitro* model [19]. The ECs which are essential in the blood vessel have been demonstrated to be aligned and elongated according to the direction of shear flow. Researchers investigated the cell adhesion and orientation of ECs in microfluidic channels with different structures such as flat and micro-patterned. The cells were also aligned in the microfluidic channel according to the flow direction. Cell alignment and elongation are considered to be an adaptive procedure of ECs to decrease the local mechanical load and consequent damage. Lee et al demonstrated that ECs aligned in the direction parallel to applied shear stress under flow, while the vascular smooth muscle cells aligned perpendicular to the flow direction [20]. Conway DE's group also confirmed that endothelical cells exposed to 15 dyn/cm^2 of shear stress for 24 h produce elongated cells that are aligned with the direction of shear stress[21]. In addition, they applied reversing shear stress to mimic the hemodynamic conditions at the wall of the carotid sinus; ECs were not aligned and were similar to cells at static condition as shown in Figure1-2. These investigations indicate that unidirectional flow shear stress induces cell orientation parallel with the direction of flow, andthe cell orientation would change according to the direction of flow.

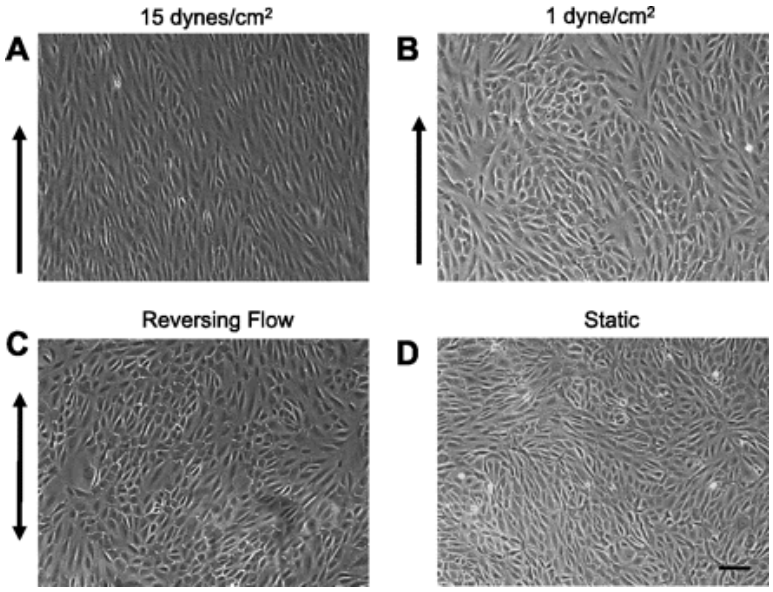

Figure 1- 2: Variations in fluid flow patterns cause altered endothelial cell (EC) morphology. *A*: phase-contrast images of ECs exposed to 15 dyn/cm2 of shear stress for 24 h produce elongated cells that are aligned with the direction of shear stress. *B–D*: ECs exposed to 1 dyn/cm2 (*B*) and ECs exposed to RF (*C*) are not aligned and are similar to the morphology of cells grown under static conditions (*D*) [21]. Arrows indicate the direction of flow. Scale bar = 100 μm.

Researchers further investigated the molecular mechanisms of ECs response to fluid shear stress. A variety of published literatures implicate integrin in cellular responses to flow. Flow can induce quick remodeling of focal adhesion contacts which indicates these locations of cell attachment may be important in mechanotransduction. Eleni Tzima et al reported that fluid shear stress is a critical determinant of vascular remodeling and atherogenesis [22]. They showed that shear stress rapidly stimulates conformational activation of integrin αvβ3 in bovine aortic ECs, meanwhile increase its binding to extracellular cell matrix (ECM) proteins [22]. They defined the role of integrin and Rho in a pathway leading to EC adaptation to flow [activation of integrins in endothelial cells by fluid shear stress mediates Rho-dependent cytoskeletal alignment]. Berne's group developed a FRET tension biosensor to understand the VE-cadherin and PECAM-1

responses to flow [23]. They found that flow induced an increase in tension across junctional PECAM-1, while a rapid decrease in tension across VE-cadherin [23]. For cultured ECs, it has been well established that fluid shear stress significantly influence the EC orientation, regulated in part through tyrosine kinase, intracellular calcium, and cytoskeleton-related pathways [24].

1.3 Cyclic strain affects the cell behavior

Besides fluid shear stress, strain is another common mechanical stimulus exist *in vivo* condition. ECs in the blood vessels are physiologically exposed to cyclic strain due to pulsatile changes in blood pressure. Similar to fluid shear stress, mechanical strain can also regulate the alignment of ECs *in vitro* with cell orienting perpendicular to the direction of uniaxial strain. In recent years, various cell stretchers have been fabricated to stretch the cells in the chamber and meanwhile observe the live cells under the microscope. The stretch direction can be uniaxial, biaxial and equibiaxial, different strain direction induce different cell orientation. A uniaxial cell stretching device was developed to investigate the realignment of cell morphology and F-actin CSK under cyclic stretch with in situ subcellular live-cell imaging [25]. Biaxial or multi-axial cell stretching devices were built in order to more closely mimic the complexities of strains occurring in vivo [26]. They found that the cyclic deformation of the cells triggered a reversible reorientation perpendicular to the direction of the applied strain. Another cyclic stretch system named Flexcell has been extensively used in mechanobiology research [27].

Mechanical strain has been reported to regulate the cell alignment, cell proliferation and differentiation [28], collagen production[29], DNA synthesis [30], and synthesis of cytoskeleton and tubulin[31]. A. Ignatius*et al.* found that mechanical strain promotes the proliferation and differentiation of osteoblastic precursor cells and the application of mechanical tension provide a beneficial effect on in vitro tissue formation [32]. Shu Chien *et al.* found that mechanical stimuli on endothelial cells effect the signaling

transduction and gene expression [28]. Although the effect of mechanical stimuli to cells has been widely investigated, the effect of strain on cellular uptake of nanoparticles has seldom been reported. In my study, we investigate the cell uptake of nanoparticles under mechanical stimuli.

1.3.1 Nanoparticles as drug carrier

In recent decades, nanoparticles (NPs) have been rapidly investigated due to its extraordinary application in medicine and more specifically drug delivery [33]. NPs are particles at sub-micrometer scales from 1 to 100 nm. NPs as drug carriers protect the drug from rapid degradation or clearance and enhance specific targeting and delivery efficiency with higher drug concentration in target tissues[34]. NPs are generally made of two parts, the core material and a surface modifier that can be used to alter the chemical properties of the core material. The core materials are usually chemical or biological materials such as polymer, silica, metals, lipids, peptides, dendrimers, or dextran. The functionality of NPs can be changed by attaching specific chemical compounds to the surface. The application of NPs depends on the chemical characteristics of the core materials and the surface modifiers. The functional surfaces are able to adsorb, bind and carry other chemical compounds such as probes, proteins and small molecule drugs by covalent bonds or adsorption. Their biocompatibility and biodegradation are determined by the core composition and surface modifiers of NPs.

Therapeutic agents integrated with NPs with optimal sizes, shapes and surface properties to prolong their circulation time, and reduce their immunogenicity. By adding targeting

ligands such as peptides, antibodies and small organic molecules onto the surface of NPs, the NP engineered therapeutic agents can specifically target cancerous cells via selective binding to the receptors on their surface[35]. With the rapid growth of nanotechnology, the toxicity of NPs attracted increasing attention for the application in drug delivery and more specifically cancer therapy. The potential toxicity greatly depends on the actual component of the NPs. When nanoparticles serve as drug carriers, they directly interact with tissues and cells in human body, which could potentially cause undesirable biological responses. Various nanocarriers have been tested as drug delivery systems, such as magnetic nanoparticles, silica, solid lipids, carbon materials or polymers. Gold (Au) nanoparticles (AuNPs) which are unique from other biomedical nanomaterials exhibit a combination of physical, chemical and photonic properties provide a multifunctional platform for site-specific drug delivery [36]. AuNPs have been reported to have better binding affinity to a particular disease type than liposomes or poly (lactic-co-glycolicacid) nanoparticles [37].

1.3.2 Cellular uptake of nanoparticles

NPs have been increasingly used as drug delivery systems for therapy, in diagnostics and in imaging. They bring great advantages by tuning their characteristic properties, such as a reduction of side effects by targeted manipulation and enhancement of detection sensitivity. Despite these advantages, we also need to consider the disadvantages they may cause. When releasing into the environment, some hazardous effects on human or environment health may occur. Adverse effects of NPs have been investigated at the cellular level, including apoptosis, toxicity, the generation of reactive oxygen species and

change in cell morphology by incubation NPs with cells. Unfortunately, the uptake mechanisms in detail of most cell toxicity studies haven't been determined. As we know, toxicity is mainly determined by the entrance pathway and the final intracellular quantity and localization. Katja Kettler *et al.* demonstrated that cellular uptake of NPs depends strongly on NP size, NP shape, degree of (homo-) aggregation and surface charges [38]. Increasing surface charges, either positive or negative, will increase particle internalization compared to uncharged NPs. The recent advance in mechanobiology have established that mechanical cues modulate many cell responses, though such modulation is cell-type dependent. In particular, substrate geography, substrate stiffness, shear flow and cyclic strain have been shown to be a regulatory factor for cell spreading, orientation, proliferation and differentiation. It has been reported that stiffness-regulated cell responses also modulate NP uptake kinetics, and this phenomenon could be utilized as a new avenue to optimize NP designs for more effective in vivo deliver. Huang's study found that a stiffer substrate results in a higher total cellular uptake on a per cell basis, but a lower uptake per unit membrane area [39]. In our study, we investigate the effect of substrate geography, shear flow and cyclic strain on cell responses, including the cell alignment, spreading, adhesion, deformation and cellular uptake of NPs.

1.3.3 Cyclic stretch influence the cellular uptake of nanoparticles

The potential use the nanoparticles as imaging, diagnostic, and drug delivery agents have raised questions about their potential for cytotoxicity. Many researches have investigated the effects of NPs on cell viability due to many recent developments utilizing NPs for pharmaceutical and biomedical applications. Megan S. Lord *et al.* synthesized rhombohedral-shaped cerium oxide nanoparticles (nanoceria) and examined the internalization ability of the nanoceria by human monocytic cell line, U937, and scavenge intracellular ROS [40]. Jillian and colleagues investigate the effects of applied strain on QD uptake by human epidermal keratinocytes (HEK) [41]. They incubated HEK cells on collagen-coated Flexcell culture plates with QD at a concentration of 3 nM and applied 10% average strain to the cells. Their results indicate that addition of strain results in an increase in cytokine production and QD uptake, resulting in irritation and a negative impact on cell viability [41]. Another study investigated the uptake of amorphous silica nanoparticles in primary endothelial cells (HUVEC) cultured under physiological cyclic stretch conditions (1 Hz, 5% stretch) and compared this to cells in a standard static cell culture system [42]. Their results indicate that cytotoxicity to endothelial cells caused by silica nanoparticles is not obviously changed under stretch compared to static culture conditions. To better understand the relationship between the cyclic stretch and the cellular uptake of NPs, we incubated endothelial cells with NPs and stretched with different strain level from 5% to 15% which mimic the strain level inside the blood vessel. The cell viability and detachment of cells under stretch have also been investigated compared to the cells in a static condition.

Chapter 2 - Enhanced cell adhesion and alignment on micro-wavy patterned surfaces

2.1 Abstract

Tons of Micro-patterns have been developed to regulate the cell behavior when cultured in vitro. General micro-patterns usually have shape comers which limit the cell spreading and cell-cell interactions. In this study, we proposed a micro-wavy pattern with smooth surface which favors cell growth on the substrate. To characterize cell growth and responses on the micro-patterned substrates, bovine aortic endothelial cells were seeded onto surfaces with micro-grooves and micro-waves for 24 h. As a result, the cells on the micro-wavy pattern appeared to have a lower death rate and better alignment compared to those on the micro-grooved pattern. In addition, flow-induced shear stress was applied to examine the adhesion strength of cells on the micro-wavy pattern[43]. The cells on the micro-wavy pattern have stronger adhesion strength than those on the micro-grooved-pattern. The combination of increased alignment, lower death rate and enhanced adhesion strength of cells on the micro-wavy patterns will offer advantages in potential applications for cell phenotype, proliferation and tissue engineering.

2.2Introduction

Valuable efforts have been made to fabricate various nano/micro-patterned substrates for application in biomedical systems in recent years [44-47]. Various factors such as surface chemistry, feature geometry and elastic modulus influence the behaviors of cells on a substrate [1]. Harrison first investigated the behavior of embryonic cells [48].Weiss named cells movement and orientation behavior as 'contact guidance' [49]. The cell behavior and morphology on silica substrates of various topology was examined by Curtis and Varde [50].During the past five decades, researchers widely investigated the topographical control of cell behaviors [51-53]. It has become increasingly important to control the position of cells in an organized pattern on a substrate for the development of cellular biosensor technology and tissue engineering applications [5-7, 54].

Cells are often organized in a particular pattern in tissue engineering, such as those in a neural network [55] and in a liver system [56]. In last decades, there have been progresses of growing a biomimetic tissue in microfluidic devices, namely "tissue-on-a-chip". Numerous methods are utilized to locate cells into a pre-designed functional pattern, such as physical and chemical cell trapping [57, 58], substrate topography [59], fluid shear [60], and compression [18]. Liu *et al.* fabricated a chip that can shape several thousands of cells into an artificial liver [61]. Electrophoresis is applied to organize particular liver cells (hepatocytes) into chains radiating from a central point [61].

With the development of nanofabrication techniques, the influences of nano-scale grooved patterns on cell spreading, alignment, morphology, and proliferation has been

investigated [8-10]. Recent researches have reported that cell orientation and differentiation can be affected by a nanostructured surface [11]. Peterbauer's group indicated that cell orientation follows the orientation of initial protrusions from the cell when seeded onto a nano-grooved surface [11]. At the same time, Wang et al. found that submicron grooved pattern inhibited proliferation of skeletal muscle cells, yet enhanced its differentiation ability [13]. Their results also supported others' studies that cells align along the grooves of the substrates. However, since the groove dimensions are much smaller than the cell size, nanogrooves cannot offer a good control of cell position. It is anticipated to use a micro-pattern with size similar to the cell in order to precisely regulate the cell location.

Many researches have been developed to investigate the effects of PDMS micro-patterned substrates geometry on cell spreading, migration and alignment [14-16, 62]. For instance, Fu *et al.* reported that the spacing and height of micro-grooved substrate can affect the spreading and adhesion of human osteosarcoma (HOS) cells [17]. Culturing HOS cells on micro-grooved substrate with spacing ranging from 5 μm to 120 μm indicates that cells orient well along the directions of microgrooves when the groove spacing is similar to the spreading size of cells [17].

There is no technique that can provide good control of both cell position and orientation while allowing for cell-cell interaction so far. In this study, we fabricated micropatterns with sinusoidal waves and investigated adhesion and alignment of BAECs on the curved surface. While most current studies focus on a flat surface, cells are usually

interacting on a non-flat surface. For example, in capillary vessel with a diameter of 5-10 μm [63], the endothelium cells are found covering a highly curved surface. It raises a fundamental and interesting question how surface curvature cue may determine cell behaviors. A lot of artificial implants also have micropatterns on the surface. For example, human umbilical vein endothelial cells were seeded onto 4 mm I.D. expanded poly(tetrafluoroethylene) (e-PTFE) grafts [64]. Understanding how cells interact with a curved surface is also essential for enhancing cell seeding and growth on these artificial materials.

This paper presents the results of an experimental study of the spreading and adhesion of cells on wavy surfaces in comparison to grooved and flat surfaces. We first fabricated smooth micro-wavy patterns with 20 μm wavelength and 6.6 μm height, and micro-grooved patterns with 20 μm spacing and 5 μm height. Then, cell spreading, alignment and death were investigated through microscopy after a 24 h incubation period. Finally, we packed a microfluidic device and place the cells in the device, then apply shear flow to the device to examine the adhesion strength of BAECs on the micro-wavy pattern compared to that on the flat and grooved surface. The implications of the results are then discussed for the application as a tissue scaffold pattern.

2.3Materials and Methods

To characterize cell growth and responses on a micro-patterned substrate, Bovine Aortic Endothelial Cells (BAECs) were seeded onto micro-groove (Figure 2-1 A and D) and micro-wavy (Figure 2-1 B and C) substrates.

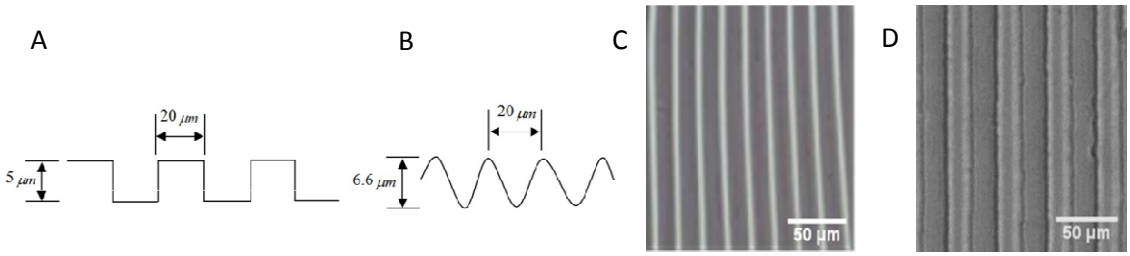

Figure 2- 1: Geometry of micropatterns. (A) Micro-groove cross-sectional figure; (B) Micro-wave cross-sectional figure; (C) 1D 20 μm wavelength wavy pattern; (D) 1D 20 μm groove length groove pattern

2.3.1 Micro-patterned PDMS substrates fabrication

Microgrooved surfaces used in cell capture or particle isolation can be fabricated through standard photolithography, followed by PDMS molding techniques [24]. However, these surfaces typically have sharp corners, which are not favorable for cell seeding, spreading, and adhesion [16, 17]. To fabricate a smooth microwavy surface, we used bucking of oxide/PDMS bilayer, as shown in Figure 2-2.

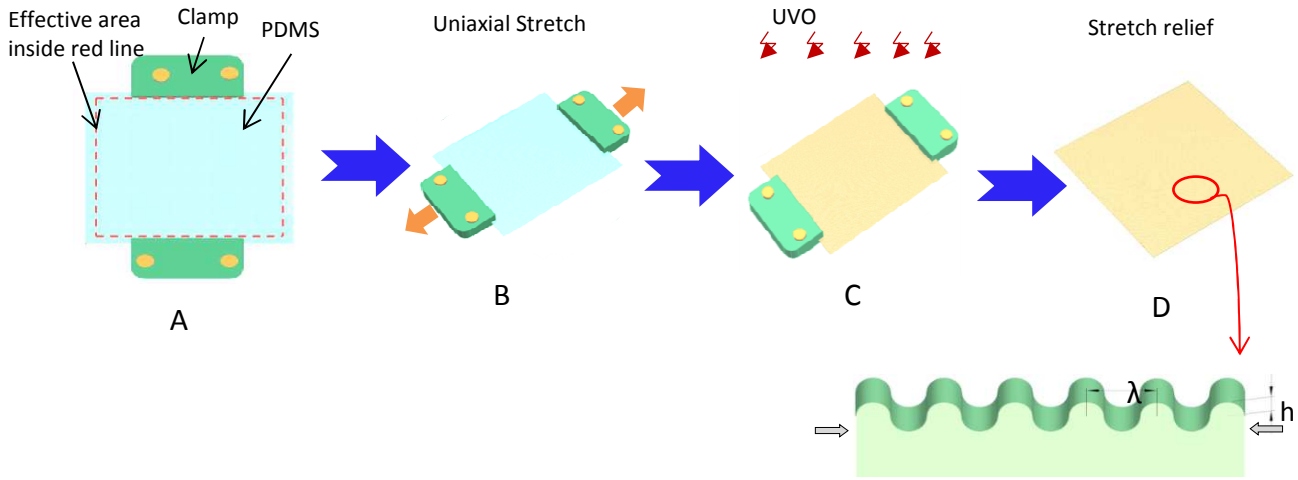

Figure 2- 2: Illustration of the fabrication process of micro-wavy patterns.(A-D) Uniaxial stretching of PDMS films at various mechanical stretch settings to generate micro-wavy patterns

Basically, a flat 0.5 mm thick PDMS sheet (40mm × 15mm) was prepared from Sylgard 184 (Dow Corning, Midland, MI, USA) in a 10:1 weight ratio of silicone elastomer base to the curing agent. After curing at 65°C for 4h, the crosslinked PDMS sheet was then uniaxially stretched by a custom-designed stretching device to 50.0% strain and exposed to a UVO cleaner (model 144AX, Jelight Company, Inc.) or O_2 plasma (Enercon Industries Corp., Menomonee Falls, WI, USA) for 1 hour to generate a thin silicate layer [65, 66]. After releasing the substrate from the stretcher, the difference in elastic modulus causes the oxide/PDMS bilayer to buckle and form wrinkled surface. The wavelength (λ) and amplitude (A) of the wrinkles can be tuned by varying the elastic modulus of the PDMS substrate and the thickness of the top silicate layer [66-69]. The micro-wavy pattern used in this study was created with a wavelength of 20 μm and a height of 6.6 μm.

We also fabricated micro-grooved molds on silicon wafers through photolithography with geometries shown in Fig. 1 D. PDMS was then poured into the

molds. After degassing in vacuum chamber for 30 min, the samples were cured in an oven at 65^{o}C for 4 hours. The cured PDMS layers were peeled off. The micro-grooved patterns were created with 20 μm spacing and 5 μm height.

2.3.2 Microfluidic device fabrication

The microfluidic shear devices were assembled by covering the fabricated micropatterned wavy surface with a PDMS transparent cover pattern. A desktop digital craft cutter (Silhouette America, Inc., UT, USA) was used to make the cover pattern [70]. By using the interactive computer software, 120 μm thick adhesive gold foil (Silhouette America Inc., UT, USA) was printed to form the design of the structure. This foil was stuck onto the glass as a cover pattern mold. PDMS was poured onto the mold. The cured PDMS layers were peeled off after 4h at 65^{o}C. The cover pattern was a rectangle 36 mm long and 6 mm wide. Two 2 mm diameter holes were punched on the two sides of cover pattern as the inlet and outlet. The PDMS substrate and cover pattern were both rinsed in 70% ethanol, plasma treated for 90 seconds, and then bound together to assemble microfluidic channel devices.

2.3.3 Cell culture on micro-patterned substrates

All reagents and chemicals for cell culture and detachment were purchased from Sigma-Aldrich USA. Our endothelial cells were obtained from Cell Applications (San Diego, CA). BAECs were maintained in 25 cm^2 cell culture flasks that were kept at 37°C in Dulbecco's Modified Eagle's medium (DMEM) containing 10% heat inactivated Fetal

Bovine Serum (FBS) and 1% Penicillin/Streptomycin in a 100% humidity atmosphere with 5% CO_2. BAECs between passages 10-15 were used in all reported experiments.

Prior to static cell culture experiment, the PDMS substrates were sterilized by rinsing with 70% ethanol (2 h), followed by phosphate buffered saline (PBS) (5 min) and autoclaved for 1 h. Gelatin was used in this study to increase cell attachment to substrate. It was diluted to desired concentration (0.2%) with TE buffer. The micropattern surfaces were rinsed with 0.2% gelatin for 2 h in the incubator to allow sufficient gelatin adsorption onto the underlying PDMS surface. After rinsing with 1ml PBS, micropatterns were rinsed and maintained in supplemented medium until cell seeding.

The cells were harvested using trypsin after reaching approximately 80% confluency. Cells were centrifuged and resuspended in Dulbecco's modified Eagle medium (DMEM) (Sigma Aldrich) with 10% heat inactivated Fetal Bovine Serum and 1% Penicillin/Streptomycin. Determined by a hemocytometer count, approximately 2.5×10^5 cells/mL concentrated cells were seeded by standard cell culture protocol onto the micro-patterned PDMS substrates. After 24 h and 48 h incubation, cell spreading and orientation was then imaged with a Nikon phase-contrast microscope with an objective magnification of 20×.

2.3.4 Imaging of cell morphology using scanning electron microscopy

BAECs were cultured on 20 μm wavy surface for 24 h. After spreading, cells were fixed in 4% paraformaldehyde for 1 h. The cells were then rinsed with PBS for 5 min (three

times). Next, the substrates were immersed into 20%, 30%, 50%, 70%, 85%, 95%, and 100% (volume/volume) ethanol concentration gradient solutions (15 min in each solution) [71]. All substrates were lyophilized in the refrigerator overnight. Cells were qualitatively examined for overall cell shape, orientation relative to the underlying waves using scanning electron microscope (SEM).

2.3.5 Cell death

Cell death was determined by staining with ethidium homodimer-1 (EthD-1) (Sigma Aldrich, USA), a fluorescent nuclear stain that penetrates dead cells and increases intensity after binding to DNA. Staining was done according to the standard procedures. Staining cells on different patterns were counted in 3 randomly selected microscopic fields (at least 500 cells) and the % positive cells were calculated relative to the total number of cells on the pattern. Cell death rate data are expressed as the mean % positive cells ± SEM.

2.3.6 Cell adhesion strength assays

Besides static seeding, cell response to external stimuli such as shear flow was also studied via a microfluidic based testing platform. A typical integrated microfluidic testing device is illustrated in Figure 2-3 A-B. The fabricated micropatterned surface was covered with a PDMS transparent cover pattern via O_2 plasma bonding [72, 73]. As a comparison, a flat PDMS microchannel device was also used as a testing device.

A B

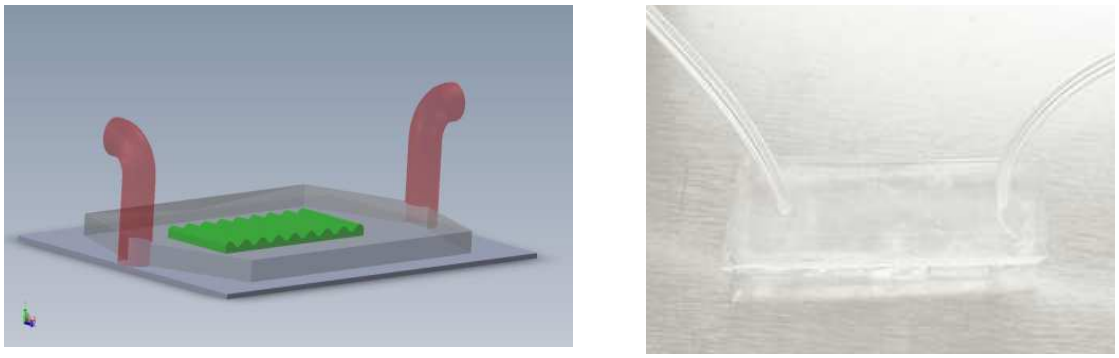

Figure 2- 3: Microfluidic based testing device.(A) Sketch of the microfluidic device; (B) Image of the microfluidic device

Cells were trypsinized from the flasks and suspended at 10^6 cells/mL [74]. To assure better cell adhesion, 100 µl gelatin was injected into the inlet reservoir of the microchannel and incubated for 2 h prior to cell culture. After rinsing with PBS, the concentrated cell suspension was injected into the gelatin-coated microchannel device using a syringe. The device was incubated at 37°C with 5% CO_2 for 1.5 h to allow initial cell attachment and spreading on the channel surfaces. Observations were made after 1.5 h incubation using a Nikon phase-contrast microscope, and images were taken with a CCD camera.

To investigate adhesion strength, attached cells were subjected to increasing levels of flow-induced shear stress over a 12 min period. Cell culture medium was driven through the microchannel by a programmable syringe pump (Harvard Apparatus PhD 2000, USA) at 2.775, 5.55, 11.1, 27.75, 55.5, 111 mL/h, each for 2min. These flow rates translated to shear stress of 0.25, 0.5, 1, 2.5, 5 and 10 dyn/cm^2. The shear stress was calculated from Equation (1) [75, 76].

$$Tw = \mu \cdot \frac{6Q}{H^2 W} \qquad (1)$$

Where μ is the viscosity of the flow fluid (0.007 g/cm/s, at 37°C), H the channel height (0.012 cm), W the channel width (0.9 cm) and Q the flow rate (mL/s). Images were taken at 2 min intervals shear period at the same place.

2.3.7 Statistical Analysis

Results are presented as means ± standard error of the mean (SEM). Statistical significance of differences was determined using Student's *t*-test.

2.4Results

2.4.1 Cell distribution

BAECs were seeded onto the wavy surface with a wavelength of 20 μm. At the initial seeding, the rounded BAECs were almost uniformly distributed on the wavy surface (Figure 2-4A). To quantify the cell distribution, the 20 μm wavelength was divided into 1 μm segment locations and a histogram of the number of cells in each segment was created (Figure 2-4B). In the phase-contrast microscope image, the white lines represent the crest of the micro-wavy surface. Most cells tend to be located at the troughs of the wavy surface, which demonstrates that wavy surfaces have good control of cell position.

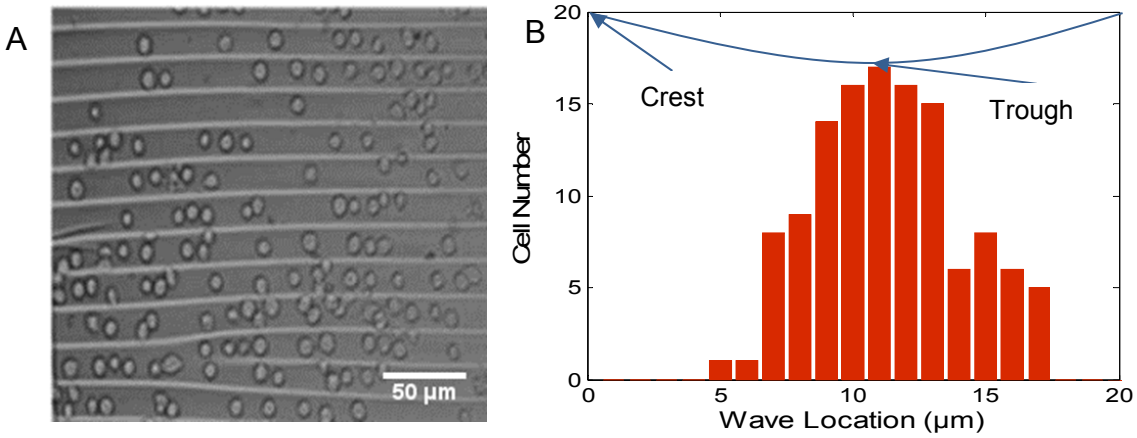

Figure 2- 4: Cell distribution at the initial seeding. (A) Microscope image of cells on a wavy surface with 20 μm spacing and 6.6 μm height; (B) The number of endothelial cells at different wave locations

2.4.2 Cell spreading, localization and alignment

After 24 h of cell culturing, while BAECs on the flat surface were randomly oriented (Figure 2-5A), those on the micro-wavy surface were found oriented along the long axis of the waves (Figure 2-5B). The BAECs on the flat surface also appeared rounder than those on the wavy surface. Comparing the images of the wavy surface captured after 24 h and 48 h (Figure 2-5B and C), no significant differences were observed on the distribution or spreading of the cells; thus, the incubation time of 24 h was utilized for further analysis. In addition, scanning electron microscopy (SEM) images revealed that the cell aligned along the wave and was located in the trough of the wave (Figure 2-5D). In preparation for SEM, cells were fixed in 4% paraformaldehyde for 1 h and washed with PBS; then, the cells were dehydrated in 20%, 30%, 50%, 70%, 85%, 95%, and 100% (volume/volume) ethanol concentration gradient solutions (each for 15 min), followed by 24 h dry out in the refrigerator. Thus in the SEM image (Figure 2-5D), cells look smaller than in the optical images because of the cell dehydration process in preparation for SEM(Figure 2-5A-C).

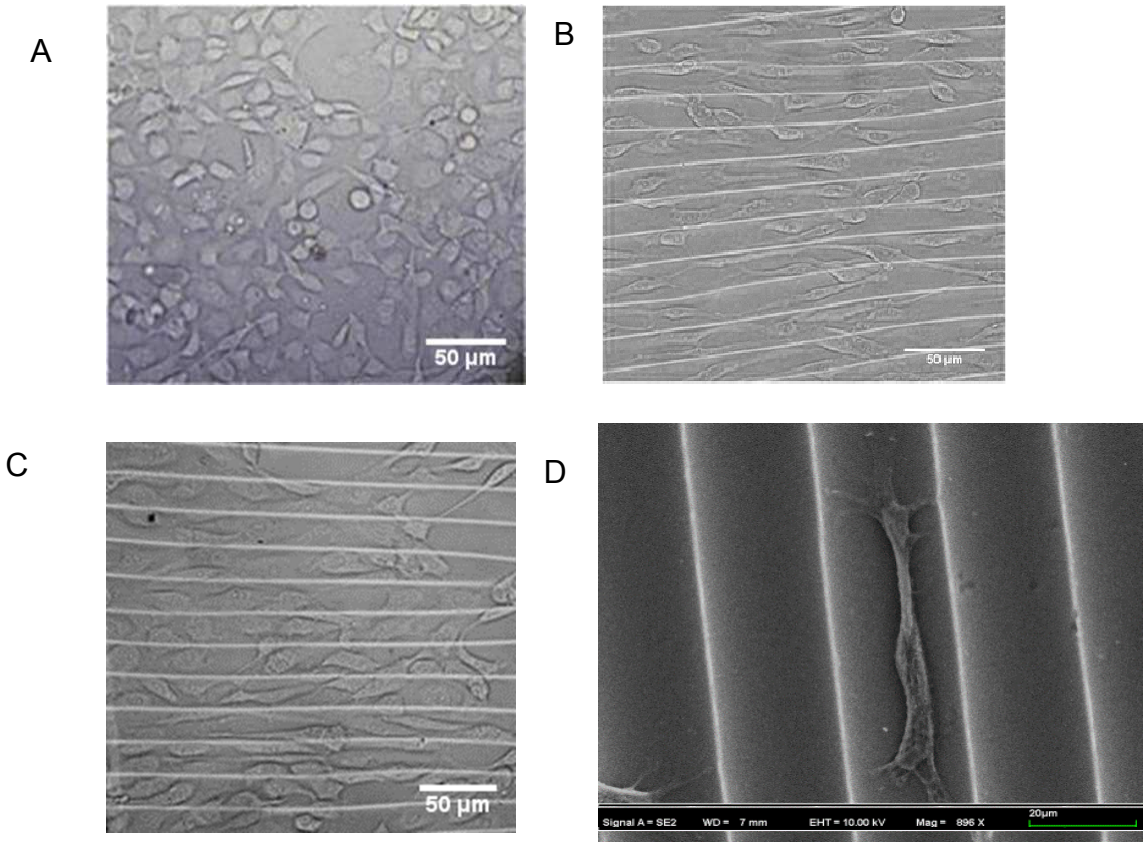

Figure 2- 5: Images of BAECs on different substrates.(A) Microscope image of cells on flat PDMS substrate after 24 h; (B) Microscope image of cells on 20 µm spacing, 6.6 µm height micro-wave after 24 h; (C) Microscope image of cells on the micro-wave after 48 h; (D) SEM image of a BAEC on micro-wavy substrate after 24 h. In Fig. D, the cell looks smaller than in Fig. A-C because of the dehydration process in preparation for SEM

The cell alignment after static seeding for 24 h was quantified using the Image J software to determine the location and alignment angle of cells. The alignment angle (0^o~90^o) of each cell was defined as the angle between the long axis of the cells and the wave direction of the wavy surface. Around 100 cells were measured after 24 h on wavy surface and a statistical analysis was performed on the measured data using Matlab.

Cells were either elongated or aligned with the wave direction or were approximately round. To quantify the cell distribution and alignment on each segment, the wavy surface was divided into peak, slope and trough three parts. The cells on the peak show better alignment than that on the slope and trough (Figure 2-6A). Meanwhile, most of the cells were found to be located at the troughs of the wavy surface (Figure 2-6B) after 24 h incubation.

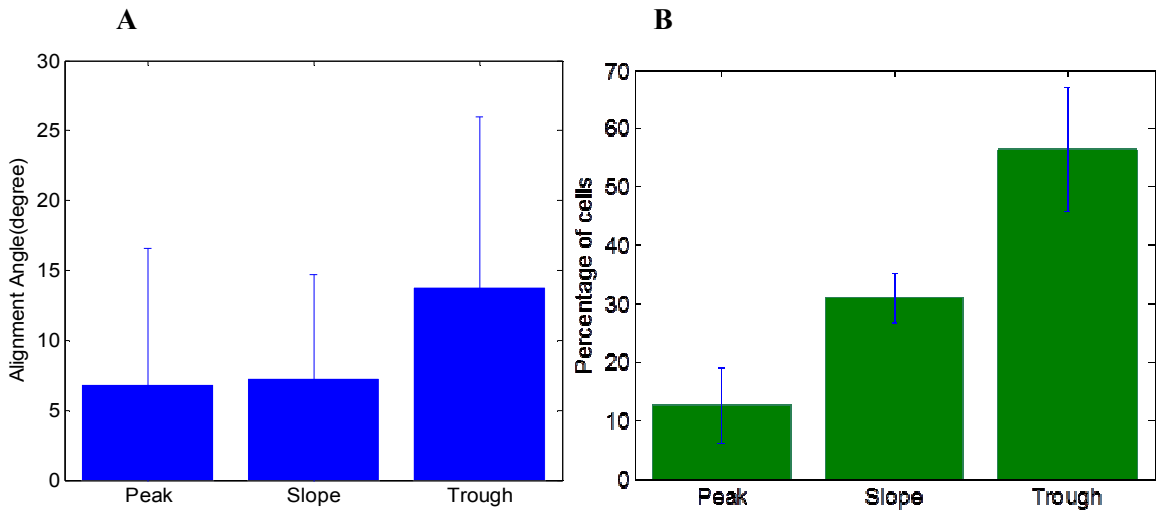

Figure 2- 6: Histogram of cell alignment (A) and distribution (B) on the peak, slope and trough of the 20 μm spacing, 6.6 μm height micro-wavy surfaces

The cell orientation histograms are presented in Figure 2-7A-C. Figure 2-7A shows that most cells were located in the troughs of the wave. Figure 2-7B shows that about 60% of the cells had a <10° alignment angle, with a significant fraction of them very close to 0° on the 20 μm wavy surface. The spread endothelial cells show strong alignment within the wavy pattern. The alignment angle and wave location of each cell are shown in Figure 2-7C. A wider angle distribution of cells is observed at troughs of the wave, while a narrow angle distribution of cells is observed at the crests of the wave.

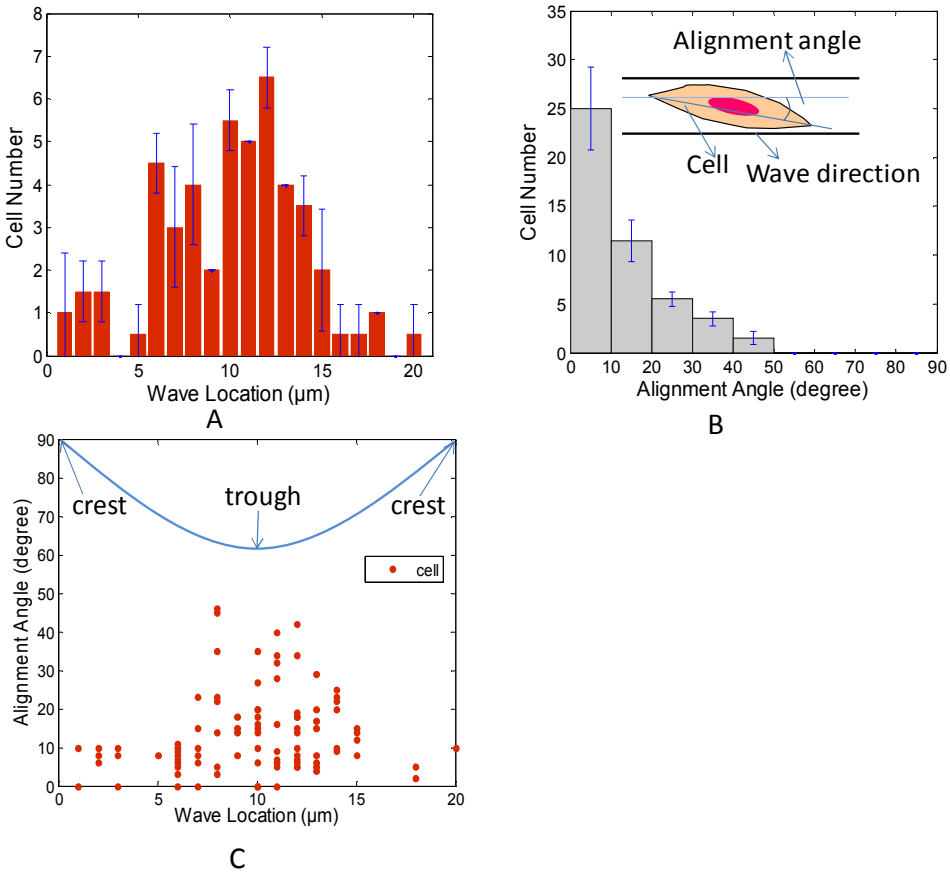

Figure 2- 7: Alignment of BAECs on 20 μm micro-wavy substrates after 24 h incubation.(A-C) Histograms of cell number, alignment angle, and cell location on 20 μm wavy surfaces (n=100). Error bars, SEM.

2.4.3 Cell spreading on micro-wavy and micro-grooved substrates

To understand surface curvature effect to cell adhesion and spreading, we seeded BAECs onto surfaces with microgrooves for comparison to those on microwaves. Similarly to the micro-wavy pattern, most of the BAECs were located at the troughs of the grooves after 24 h incubation, as shown in Figure 2-8A-B. Figure 2-8C shows that cells on the 20 μm wavy surface had better alignment than on the 20 μm groove surface.

Cells were found to not only seed denser on the wavy surface, but also spread healthier, which was quantified by the death rate of cells. Cells on a 20 μm grooved

surface had a higher death rate after 24 h than those on the 20 µm wavy pattern and flat surface as depicted in Figure 2-8D. This may be explained by the larger area exposed to the culture medium on the wavy surface compared to confinement of the grooved surface.

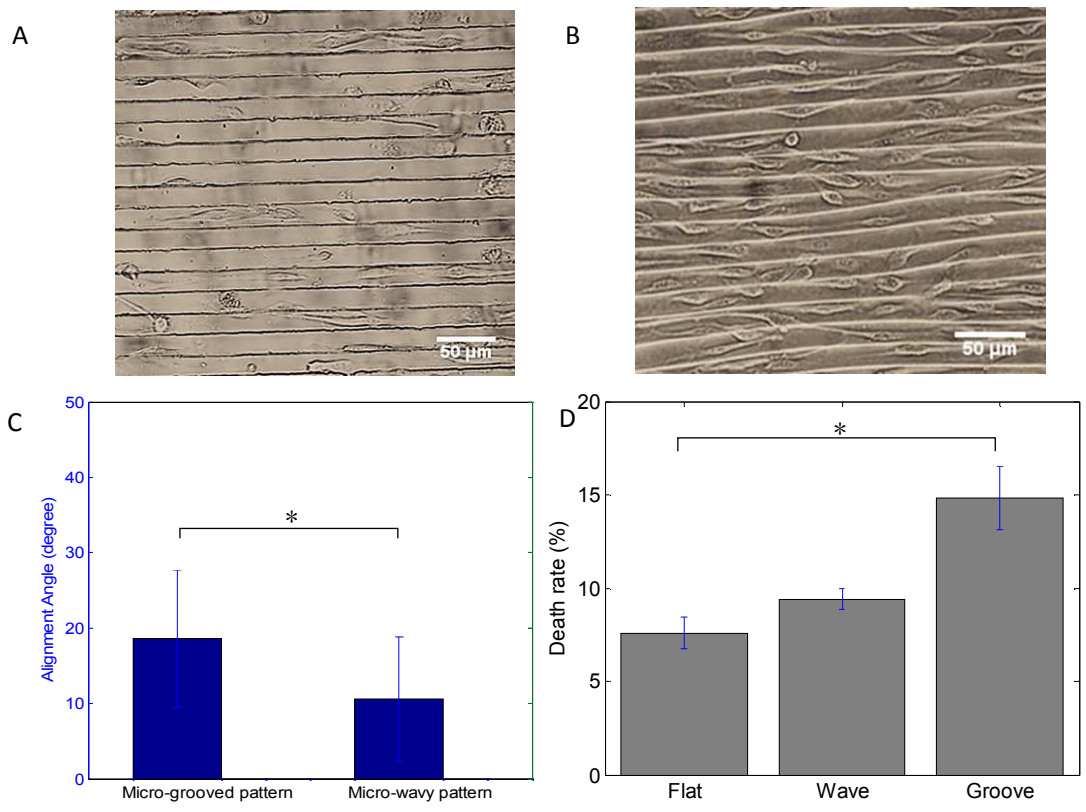

Figure 2- 8: Phase-contrast images of BAECs after 24h incubation. (A) 20 µm spacing, 5 µm height micro-groove; (B) 20 µm spacing, 6.6 µm height micro-wave; (C) Alignment angle (mean ± SEM) of BAECs on micro-grooved and micro-wavy pattern. (D) Death rate of BAECs on flat, groove and wavy surface. BAECs on the wavy pattern show better alignment and lower death rate than those on the micro-grooved pattern. *P < 0.05; Student's t test.

2.4.4 Cell adhesion strength

To measure the cell adhesion strength, five control experiments were performed to examine cells detachment over time and as a function of shear stress. The flow was applied in the direction of both perpendicular and parallel to the grooves and waves. In

the first experiment, the shear flow was fixed at 1 dyn/cm^2 for 12 min. This particular shear level corresponds to the lower end of physiological shear stress in the blood vessels which ranges from 1 dyn/cm^2 to 70dyn/cm^2 [77]. The number of attached cells decreased quickly within the first 2 min, and plateaued afterwards, as shown in Figure 2-9A. This suggested that at a given shear level cells detached quickly rather than gradually peeled off over time. Thus, two minutes is enough to establish a steady number of cell detachment.

The second experiment was performed by repeating the standard shear assay of 0.25, 0.5, 1, 2.5, 5 and 10 dyn/cm^2 at 2 min intervals over the 12 min period. We measured percentage of cells stayed in flat, groove and wavy channels at six levels of shear stress (Figure 2-9B). In total, three experiments (n = 3) were conducted for each channel with flat, groove and wavy surfaces, respectively. Qualitative evaluation of these profiles showed that BAECs were attached to flat channels with ~60% cells remaining after the assay. When the flow direction was perpendicular to the grooves and waves, BAECs attached better on wavy channel with ~80% cells remaining after the assay. While when the flow direction was parallel to the grooves and waves, BAECs on the wavy pattern channels also showed stronger cell adhesion than those on the grooves and flat ones.

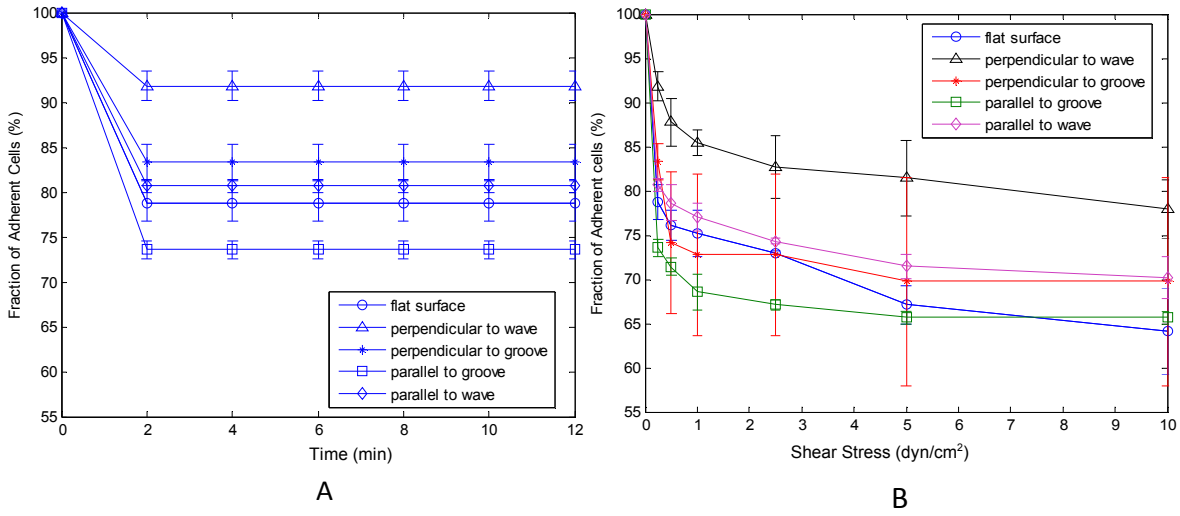

Figure 2- 9: Shear flow testing via a microfluidic based testing platform. (A) Shear stress of 1 dyn/cm^2 was applied for 12 min; (B) Diagram represents shear stress level applied, 2 min at 0.25 dyn/cm^2, 2 min at 0.5 dyn/cm^2, 2 min at 1 dyn/cm^2, 2 min at 2.5 dyn/cm^2, 2 min at 5 dyn/cm^2, 2 min at 10 dyn/cm^2. Data presented as mean ± SEM (n=3).

2.5Discussion

The scaffolds used for tissue implantation have requirement of geometries which favors cell attachment, differentiation and proliferation. This study particularly analyzed the cell adhesion strength on different substrate geometries which is important for cell seeding on scaffolds as the cells must be able to withstand the local shear stresses in a dynamic in vivo system. In this study, a 20 µm periodic wavy pattern was indicated to significantly enhance BAECs orientation and adhesion compared to a flat surface, as shown in Figure 2-6 and Figure 2-9.

It is widely investigated that micro patterning has the ability to modulate the cell morphology, function and its application in tissue engineering. Fu et al. [17] found that the cells align well along the directions of microgrooves when the groove spacing is

comparable to the spread cell size. Their results are consistent with the results obtained from the cell alignment on micro-wavy and micro-grooved PDMS substrates, as shown in Figure 2-8A-C. In this work, stronger alignment effect and lower death rate were observed for cells on the micro-wavy pattern compared to that on a micro-grooved pattern.

ECs culture *in vitro* is usually executed under static conditions such as in a culture dish or flask with stationary medium [78]. Since endothelial cells form the inner lining of blood vessels, they are normally exposed to continuously flowing blood as opposed to static conditions. It is therefore desirable to study the cell/biomaterial interactions *in vitro* under conditions closely resembling those *in vivo*, specifically under shear stress after seeding [79]. The results indicated that BAECs on wavy surface had stronger adhesion strength than cells on flat and groove surface (Figure 2-9B). This might be due to the concave shape of the wavy pattern, leading to larger contact area with cell, which is favorable for cell adhesion.

It has been reported that traditional two-dimensional (2D) tissue culture is less physiological than three-dimension (3D) tissue culture [80-83]. Chen *et al.* described experimental scenarios in which 3D culture is particularly relevant, highlight recent advances in materials engineering for studying cell biology, and discussed examples where studying cells in a 3D context provided insights that would not have been observed in traditional 2D systems [83]. Usually a complex setup using ECM matrix and tracker is needed for such 3D study. Here, the wavy surface with tunable surface topography might

allow us to study cell adhesion in a semi-3D environment, which is more cell friendly than a flat and groove surface.

2.6Conclusions

A micro-wavy pattern has been proposed to influence both the initial seeding and orientation of cells. Most cells are found to stay in troughs of the wavy pattern, which is similar to that on the groove pattern. Meanwhile, BAECs on the micro-wavy pattern demonstrate lower death rate than that on micro-grooved pattern. More importantly, BAECs adhered to the wavy surface, displaying both improved orientation and adhesion strength compared to that on the flat surface. Although BAECs are used in this study, the enhanced alignment and adhesion observed should be applicable to various other cell lines. Our findings suggest that this micro-wavy pattern could be utilized in cell culture for studying cell biology and in cell seeding as a tissue scaffold surface pattern to improve cell adhesion.

Chapter 3 - Cyclic strain enhances cellular uptake of nanoparticles

3.1 Abstract

Cyclic strain has been investigated to regulate the cell behavior such as cell orientation and proliferation, but little is known about the cell uptake of NPs responses to cyclic stretch. With the application of NPs as drug carriers, the cellular uptake of NPs gained more investigation. We propose to examine the cellular uptake of NPs under cyclic stretch with strain levels from 5% to 15% which mimic the strain level in the human vessel. BAECs were cultured on collagen-coated Flexcell culture plates and placed under cyclic equal-axial strains. NPs of sizes from 50 to 200 nm were loaded at a concentration of 0.02 mg/mL and cyclic strains from 5 to 15% were applied to the cells for one hour. Results indicate that the enhanced uptake also depends on size of the NPs with highest uptake by 100 nm NP. The effect of enhanced NP uptake lasts around 13 hours after cyclic stretch. Such in vitro cell stretch system mimics physiological conditions of the lung vessel and could potentially serve as a biomimetic platform for drug therapeutic evaluation.

3.2 Introduction

In recent years, rapid progress has been made in nanoparticle (NP) technologies for the development of disease diagnosis and therapy [84]. It was found that cellular uptake of NP efficiency and quantity depends on various nanoparticle characteristics, including the NP concentration [85], size [86], shape [87], and surface chemical structures [88]. However, these discoveries have not yet been applied to effective targeted therapies due to the complexity of the *in vivo* environment that severely inhibits their efficiency. This must be overcome to fully exploit the potential of NPs to improve drug pharmacokinetics and pharmacodynamics.

It is obvious that ECs form the interior of the blood vessels and serve as a major barrier for therapeutic agents passing through the bloodstream to the target tissues [89]. NPs can serve as carriers of drug for targeting therapeutic to specific location and enhancing the resistance time in body. [90] . NPs entrance into cells depends on various factors, such as the size of the NP, the surface coating and charge [91].For example, the efficiency of carboxydextran-coated superparamagnetic iron oxide nanoparticles (SPION) uptake was correlated to the amount of carboxyl groups on the NP surface [92]. Cationic D, L-polylactide (PLA)-NP entered Hela cells in greater amounts than anionic PLA-NP [93] . In this work, we investigate the endothelial cell uptake of carboxylated polystyrene NPs (PS-COOH) with positive charge.

Furthermore, ECs *in vivo* are obviously exposed to a variety of mechanical stresses including shear flow and cyclic strain caused by the blood flow [94]. The investigation of ECs response to mechanical stresses through *in vitro* experiments helps in the understanding of endothelial function, mechanisms involved in endothelial damage, and therapeutic targeting. It has been reported that cyclic strain influences the mechanical properties of ECs, such as cell proliferation [95], cytoskeletal structure [96], signal transduction [97], gene expression and transfer [98]. However, few researches have been executed to examine the effect of cyclic strain on the cellular uptake of NPs [99]. The goal of this study is to quantify the effects of cyclic strain on the cellular uptake of NPs and its relationship with NP. The improvement of NPs internalization by ECs under physiologically relevant mechanical stress might be valuable for the advance of targeted therapeutics.

In this work, we seeded the BAECs on Flexcell six-well plates and stretched the membrane with a cyclic stretcher to investigate the EC internalization of NPs. The aim of this study was to find out the correlation between cyclic strain and the internalization of NPs into endothelial cells. The results indicated that cyclic strain obviously increased the cellular uptake of NPs. We further examined the strain effect on the cellular uptake of NPs by altering the cyclic strain level and particle size. The results demonstrated that the enhanced cellular uptake was size-dependent with an optimal particle size of 100 nm. Additionally, the cellular uptake is strain-dependent and improves as the strain level increases.

3.3 Materials and Methods

All reagents and equipment, unless otherwise indicated, were purchased from Sigma-Aldrich USA.

3.3.1 Cell culture

The bovine aortic endothelial cells (BAECs) which provided by Cell Applications (San Diego, CA) were cultured in 25 cm^2 cell culture flasks using a medium containing Dulbecco's Modified Eagle's medium (DMEM), 10% heat-inactivated fetal bovine serum, and 1% Penicillin/Streptomycin inside a humidified incubator at 5% CO_2 and 37 ^oC [43, 100]. The cells were passaged in a split ratio of 1:2. All experiments were performed with cells between passages 10 and 15.

3.3.2 Seeding of BAECs for cyclic stretch study

Cell culture medium was aspirated from the flask and the cell monolayer was washed with sterile phosphate buffered saline (PBS, pH 7.4). After removing the PBS, 3 mL trypsin was added to the flask. The flask was placed in the incubator (Thermo scientific, USA) at 37^oC for 3 min to allow for cell detachment. Fresh cell culture medium was added to the flask and flushed with a 10 mL pipette several times to ensure that all the cells were in suspension. Afterwards the cell suspension was transferred to a 15 mL tube. The cells were centrifuged at 1500 rpm for 5 min in order to pellet the cells.

The supernatant was discarded and cells were resuspended in fresh cell culture medium. For the cyclic stretch study, BAECs were seeded into six-well, collagen type I coated Bioflex plates (Flexcell international Corp., NC, USA) at 6×10^5 cells/well, determined by a hemocytometer count.

3.3.3 NP uptake assay and cyclic stretch

Carboxylate-modified fluorescent polystyrene NPs (50 nm, 100 nm, 200 nm) were sonicated for 15 min to break apart possible aggregations and diluted to the final concentration of 0.02 mg/mL in fresh culture medium [39]. This concentration is non-toxic and can be applied without overloading the cells with nanoparticles. After cells reached 80% confluence in the six-well plates, the media was discarded and replaced with NP medium, and BAECs from the test group were subjected to cyclic stretch with frequency of 1 Hz and cyclic strain (5%, 10%, and 15%) for 1 h. A Flexcell tension system (Flexcell international Corp., NC, USA) was used to apply physiological equibiaxial cyclic strain for a wide range of durations, amplitudes, and frequencies [101, 102]. The control group was not subjected to the cyclic stretch while kept in the same condition as the test group.

3.3.4 Analysis of cellular uptake

After loading the NP for 1 h, the cells were rinsed with DPBS to eliminate free particles that were not taken up by the cells. Phase contrast and fluorescence images were acquired with a Nikon phase-contrast microscope using a 20x lens (Olympus, JP). For quantitative analysis of cellular uptake, 0.5% Triton™ X-100 in a 0.2 M NaOH solution

was added to destroy the cell membrane [86]. The cell medium was transferred to a 96-well plate. Quantitative measurement was then performed by the definite quantitative determination of each cell lysate with a fluorescence Infinite M200 Pro microplate reader (Tecan, Männedorf, Switzerland).

3.3.5 NP localization and cell viability assay

After cyclic stretch for 1 h, cells were washed three times with PBS, fixed in 4% paraformaldehyde for 30 mins, and then washed three times with PBS. Afterwards, cells were permeabilized in 0.3% Triton™ X-100 for 5 mins at room temperature. Cells were washed three times with PBS and then incubated with DAPI to visualize nuclei. Cells viability was determined by staining the cells with Calcein AM. The fluorescence images were observed under a Nikon phase-contrast microscope with 20 × objective.

3.3.6 Statistical analysis

The cellular uptake of nanoparticles (%) was calculated as the fluorescence of the NPs taken up by the cells relative to the total fluorescence of the NPs in the solution. Results are expressed as means ± standard error of the mean (SEM). Statistical analysis was conducted by using the Student's *t*-rest, with $P < 0.05$ as the significant difference. Each data point were performed with a minimum of three independent experiments (n=3).

3.4 Results

3.4.1 Size-dependent uptake of NPs

In this study, nanoparticles of different sizes 50 nm, 100 nm, and 200 nm were used to evaluate the correlation between particle sizes and the internalization of NPs into endothelial cells. The fluorescent dye embedded inside the NPs allows us to quantify cellular uptake through fluorescence images. Assuming that the fluorescence intensity is proportional to the number of fluorescent NPs, the average fluorescence yielded within individual cells indicates the cellular uptake of NPs. It should be mentioned that in extracting the fluorescence intensity, the seeded cells were extensively washed using DPBS to remove any NPs adhered to the cell surface. Therefore, the fluorescence intensity accounts only for the internalized NPs. The cells were cultured in six-well plates for 24 h before loading the NPs for 1 h. We further quantify the cellular uptake of NPs with a fluorescence Infinite M200 Pro microplate reader (Tecan, Männedorf, Switzerland, λex 488 nm, λem 644 nm). As shown in Figure 3-1A, BAECs uptake more 100 nm NPs than 50 nm and 200 nm NPs. The result indicates that cellular uptake exhibited size-dependence for the NPs in BAECs, and the optimal size was around 100 nm. This result is consistent with other investigations that cells uptake more 100 nm than other sizes [86, 103].

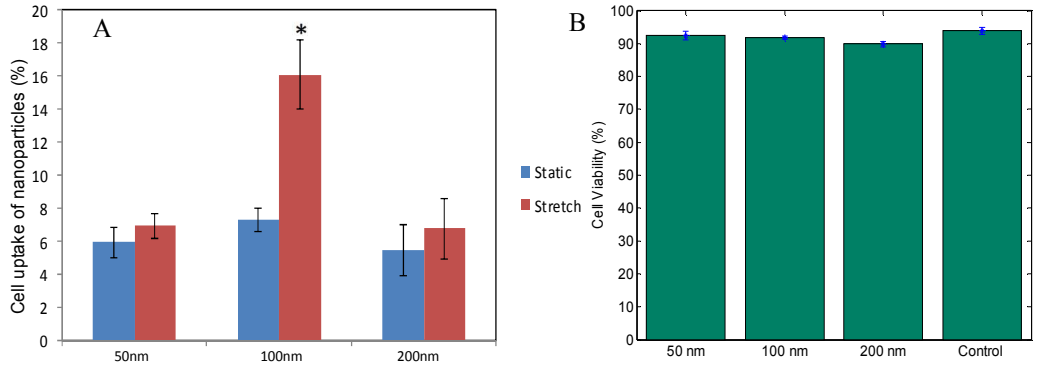

Figure 3- 1: Uptake efficiency of 50 nm, 100 nm and 200 nm particles. The uptake of 100 nm nanoparticles has significant enhancement after stretching compared to static condition. (B) Cell viability after incubation with NPs of different sizes and without NPs (control). Bars represent mean ± SEM (n=3). * Denotes significant differences ($p < 0.05$).

3.4.2 Comparison on the stretch enhanced uptake of the different sized NPs

We compared the cyclic stretch effect on 50 nm, 100 nm, and 200 nm particles uptake separately. We found that after stretching with 15% strain for 1 h, the uptake enhancement of 100 nm particles was much higher than those of 50 nm and 200 nm particles (Figure 3-1A). While 50 nm and 200 nm particles shows around 20% higher cellular uptake after stretching for 1h, 100 nm particles shows more than two folds of enhancement.

We also investigated the viability of cells with Calcein AM staining after incubation with 50 nm, 100 nm, and 200 nm NPs. The cell viability was analyzed by calculating the percentage of live cells on the substrate. Comparing with cells without NP exposure, no significant differences were found as shown in Figure 3-1B. This indicates that incubation with NPs from 50 to 200 nm does not have apparent effect on cell viability.

3.4.3 Stretch effect on cellular uptake of NPs

Since it was found that 100 nm NPs have the highest uptake in cells compared to 50 nm and 200 nm NPs, we used carboxylate polystyrene NPs (PS-COOH) with diameters of 100 nm to study the dependence of strain level on cellular uptake. BAECs were cultured on six-well plates for 24 h before loading NPs into the culture media. Fluorescence and phase contrast images were taken after loading NPs for 1 h at different strain levels (Figure 3-2).

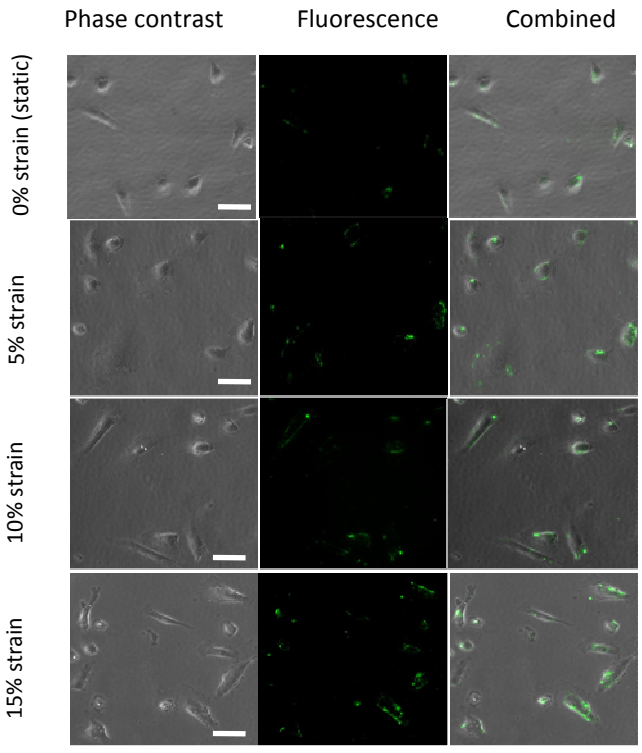

Figure 3- 2: Cellular uptake of fluorescent NPs by the cells on plates with different strain ratio (0%, 5%, 10% and 15%) (Scale bar: 20 μm). Cells were cultured on substrates for 24 h before loading the NPs. Images were taken after loading the NPs for 1h.

The images show that the stretch influences the cellular NP uptake quantity. A microplate reader was used to quantify the uptake of NPs in each plate. For each sample,

the negative control of cells without NPs was also determined. We found that the application of cyclic stretch significantly promotes the cellular uptake of 100 nm polystyrene nanoparticles relative to static cells, as depicted in Figure 3-3. This qualitative observation agrees with that reported by Huh *et al.*[104]. We further compared the cellular uptake of NPs with different cyclic strains: 5%, 10%, and 15%. Results in Figure 3-3A indicate that the cellular uptake of NPs is strain-dependent, and higher strain leads to more NP uptake. The endothelial cells *in vivo* are exposed to shear stress and cyclic stretch induced by the pulsatile blood flow. The levels of applied uniform strain (5 to 15%) cover the range of strain experienced by endothelial cells *in vivo*. This result indicates that mechanical strain influences NP uptake, which is not considered in the static culture dish work. NP uptake observed in such a cyclic strain system is closer to one that might be observed in animal studies for drug targeting and toxicology applications.

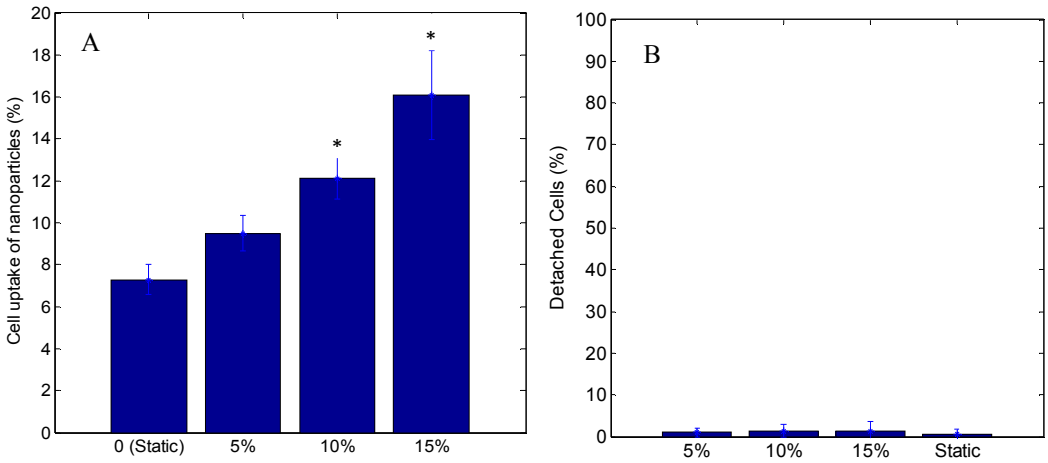

Figure 3- 3: Cell incubation with nanoparticles after stretching for 1 h with cyclic strain (5%, 10%, 15%) and at static condition (control group). (A) Cellular uptake efficiency of nanoparticles. (B) Percentage of detached cells indicates no significant detachment difference. Bars represent mean ± SEM (n=3). * $p < 0.05$ vs. static cells.

To make sure cyclic stretch doesn't get cells detached, we also examined the detachment of cells after incubation with 100 nm NPs under cyclic strain (5%, 10%, and 15%) for 1 h.

No significant difference of cell detachment were found compared to static cells as shown in Figure 3-3B, partially because the plates were coated with collagen type I which can help cell adhesion on the surface. The result indicates that the strain level from 5 to 15% will not apparently lead to the detachment of cells.

3.4.4 NPs localization within the cells

To figure out the distribution of NPs within the cell, position of the nuclei in each cell was labeled with DAPI staining. The intracellular localization of the NPs was recorded after 1 h using fluorescence microscopy. As shown in Figure 3-4, most of the NPs were located outside of the nucleus and within the cell cytosol. This result is consistent with that reported in literature [2][3]. Additionally, cyclic stretch did not change the localization of NPs within the cells as shown in Figure 3-4 B, D. NPs are still localized in the cell cytosol after stretching.

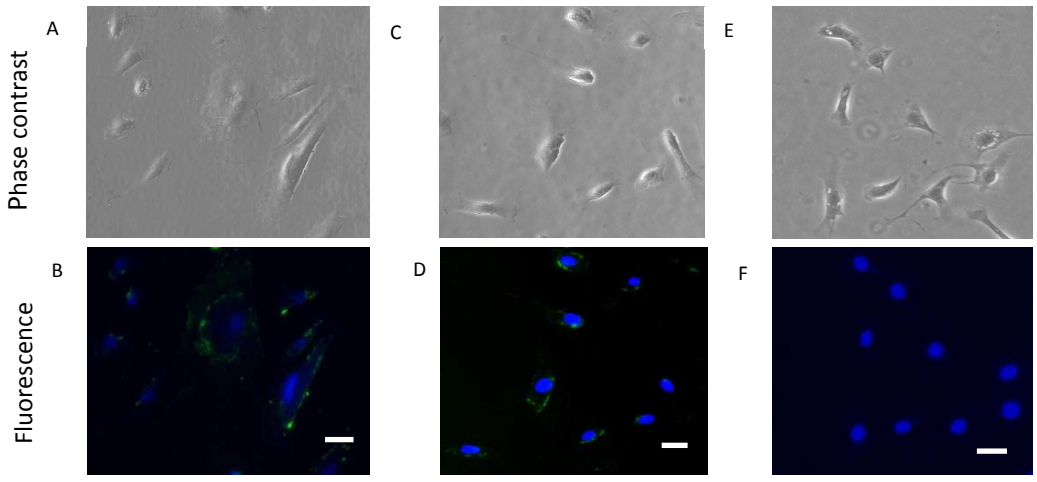

Figure 3- 4: Phase contrast and fluorescence images of BAECs after nanoparticles uptake for 1 h. (scale bar: 10 μm). The nucleus in each cell was labeled with DAPI staining (blue color). (A-B) Represents uptake of 100 nm nanoparticles by BAECs with 15% stretching for 1 h. (C-D) Represents uptake of 100 nm NPs by BAECs incubated for 1 h without stretching. Nanoparticles (green color) are seen outside of the nucleus. (E-F) Control experiment without nanoparticle incubation.

3.4.5 Time duration of NP uptake enhancement effect

We further explore how long this stretch-enhanced NPs uptake effect lasts. To investigate the effect duration time, we first stretched the cells for 1 h without loading the NPs. We then loaded the NPs into each plate after waiting for 0, 2, 4, 6, 9, 11, 13 and 22 h separately. Fluorescence signals were quantified by a microplate reader for each sample. The cells exposed to cyclic stretching uptake more NPs than the control group of cells. The NP uptake enhancement effect after stretching decreases nonlinearly with time and disappears after 13 h compared to the cells without stretching, as shown in Figure 3-5. The cellular uptake of NPs did not obviously change even 4 h after stretching and began to decrease 6 h after stretching. This result indicates that the effect of cyclic stretch on cellular NP uptake can last for as long as13 h.

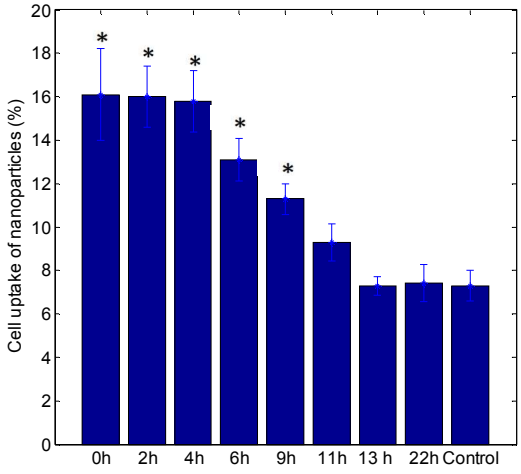

Figure 3- 5: The cellular nanoparticle uptake after stretching 1 h and waiting for 0 h, 2 h, 4 h, 6 h, 9 h, 11 h, 13 h, and 22 h. Control group shows the cells without stretching. The uptake of nanoparticles decreased after 4 h and recover to static condition after 13 h. Bars represent mean ± SEM (n=3).* $p < 0.05$ vs. control group.

3.5 Discussion

The rapid development of NPs provides great improvement in biomedical therapies due to its application as drug delivery carriers or imaging tools [105]. *In vitro* experiments were generally conducted to investigate the targeting, delivery, and uptake behaviors of nanoparticles. It is highly desirable to develop *in vitro* models that mimic the *in vivo* environment. For example, Huh *et al.* develop a biomimetic microsystem that reconstitutes the critical functional alveolar capillary interface of the human lung to investigate cell reactions such as toxicity or the formation of reactive oxygen species [104]. Compared to static culture, the addition of cyclic strain provides physiological conditions closer to that *in vivo*.

We found that BAECs uptake more NPs under cyclic strain conditions compared to static conditions and such enhancement is size-dependent and strain-dependent. To my understanding, very few investigations were previously found about the correlation between cyclic strain and NPs uptake into endothelial cells. Rouse *et al.* examined the cell viability, quantum dots (QD) uptake, and cytokine production under 10% cyclic strain condition [41]. Their results indicate that the addition of stain results in an increase in QD uptake by human epidermal keratinocytes (HEK). They reported that application of physiological load conditions can increase cell membrane permeability, thereby increasing the concentration of QD nanoparticles in cells. Other research further demonstrated that cyclic stretch leads to the generation of reactive oxygen species, which

increase monolayer permeability via activation of NF-kB and extracellular signal–regulated kinase (ERK) [106].

According to the experimental results in this work, the enhanced NP uptake effect will disappear after 13 h. This may be related to the response of cells to mechanical strains. Other studies also reported that repeated stretches resulted in the trafficking and remodeling of caveolin-3-rich membrane domains and accelerated turnover of membrane glycosphingolipids [107]. The mechanical strain effects on the cytoskeleton also play an important role in mechanotransduction [25, 108]. The changes in the arrangement of the cytoskeleton and the stretch-induced unfolding of caveolae might reflect the mechanisms of the cellular adaptation to mechanical strains which may affect endocytosis events [109]. This may result in a changed uptake rate of NPs in BAECs in a strain-dependent manner. When the mechanical strains disappear, the cellular uptake of NPs recovers to normal condition after 13 h.

The outcomes of this *in vitro* study indicate that mechanical strain influences the BAEC's ability to uptake NPs. This study has also shown that differences occur with different cyclic strains and particles sizes. More testing in the future, such as using a different endothelial cell type, strain frequency, stretch time, particle type, chemical structure, and NP concentration can be performed to better understand how mechanical strain affects the uptake of NPs into endothelial cells.

3.6 Conclusions

Mechanical strain is shown to enhance cellular uptake of nanoparticles. The cell internalization of nanoparticles is size-dependent and has an optimal size of about 100 nm. Additionally, the cell internalization of nanoparticles is strain-dependent and shows more internalization with higher strain levels. This enhanced nanoparticle uptake behavior can last for 13 h and disappears afterwards. Future research is needed to investigate the intercellular processes and activities affected by cyclic stretch to further understand the uptake mechanism. The strain level used in this study is similar to that in physiological systems, thus it may be helpful to understand targeted nanoparticle drug delivery *in vivo*.

Discussion

General micropatterns created by standard photolithography process are usually rectangular channels with sharp corners (microgrooves). So far, cells are localized on these microgrooves with sharp corners as reported in most of the researchers. While these grooves provide strong geometry constrain on cells, these individually separated microgrooves cannot provide contact interfaces between cells, which are important for cell-cell interaction study. Additionally, cells on the microgrooved substrate exhibited significantly lower proliferation rates compared to those on the flat surface [110].

A micro-wavy substrate with smooth surfaces has been fabricated to modulate the cell spreading and adhesion on the substrate. This work presents the results of an experimental study of the alignment and adhesion of cells on wavy surfaces in comparison to grooved and flat surfaces. ECs in vitro are exposed to shear flow in the blood vessel, thus it's better to investigate the cell behavior under flow condition compared to static condition. In the current study, the cells were subjected to shear stress from 0.25 dyn/cm^2 to 10 dyn/cm^2 after static spreading on both wavy, groove and flat surface. ECs cultured on the microwavy surface indicated better adhesion strength than those on the groove and flat surface.

ECs *in vivo* are constantly exposed to a variety of forces that generate mechanical stresses within the human body including shear stress, hydrostatic pressure, and cyclic strain

caused by the pulsatile blood flow [94]. Significant efforts have been made in the design of surface functionalized and bioconjugated NPs [111]. Recent studies have focused on targeting the endothelium with NPs as therapeutic agents for a variety of targeted therapeutics because of the large population of ECs in the tissue and blood flow [112]. Nanoparticles (NPs) can serve as containers for the targeting of therapeutics to specific location and increasing the resistance time in the body [90]. However, very few researches have been studied to examine the effect of cyclic strain on the cellular uptake of NPs[99]. Our study investigated the effects of cyclic strain on the cellular internalization of NPs. The main outcome of our study was that under cyclic strain conditions, more carboxylate polystyrene NPs were internalized by BAECs compared to static cell culture conditions and such enhancement is NP size and strain level dependent. The improvement of NPs internalization by ECs under physiologically relevant mechanical stress might be valuable for the advance of targeted therapeutics.

Conclusions and outlook

In this work, both substrates with patterns and mechanical forces such as shear flow and cyclic strain [113] have been applied to investigate the corresponding cell behavior including cell spreading, alignment, adhesion, deformation and uptake of NPs. In order to further measure the strain on the cell surface, a molecular sensor can be built to probe the deformation of cells. This study helps us understand how cell sense and response to mechanical stress and also provide a potential to measure the strain level on cells.

A micro-wavy pattern has been fabricated to regulate both the initial seeding and orientation of cells. Most of cells are found to locate in troughs of the wavy pattern, which is similar to that in the groove pattern. In addition, BAECs on the micro-wavy pattern indicate lower death rate than that on micro-grooved pattern. What's more, BAECs adhered to the wavy surface, displaying both enhanced alignment and adhesion strength compared to that on the flat surface. Although BAECs are used in this study, the improved adhesion and orientation observed should be applicable to various other cell lines. This study advises that this micro-wavy pattern could be applied in cell culture to understand cell biology and in cell seeding as a tissue scaffold surface pattern to enhance cell adhesion.

Mechanical strain has been applied to investigate the cellular uptake of NPs in my study. The cyclic strain is demonstrated to improve the cell internalization of

nanoparticles. The cell uptake of nanoparticles is size-dependent and shows an optimal size of about 100 nm. What's more, the cellular uptake of nanoparticles is strain-dependent and indicates more internalization at higher strain levels. The increased nanoparticle uptake phenomenon can stay for 13 h before disappear. In order to further understand the internalization mechanism, future study is acquired to inspect the intercellular processes and activities influenced by cyclic strain. The strain ratio applied in this work is similar to that in physiological systems, thus it can help us understand targeted drug delivery of NPs *in vivo*.

References

1. Martínez, E., et al., *Effects of artificial micro- and nano-structured surfaces on cell behaviour.* Annals of Anatomy - Anatomischer Anzeiger, 2009. **191**(1): p. 126-135.
2. Kawashima, T., et al., *Feasibility study on cellular network analysis with patterned cell culture microdevice.* Microelectronic Engineering, 2010. **87**(5-8): p. 704-707.
3. Huh, D., et al., *Microengineered physiological biomimicry: Organs-on-Chips.* Lab on a Chip, 2012. **12**(12): p. 2156-2164.
4. Roth, E.A., et al., *Inkjet printing for high-throughput cell patterning.* Biomaterials, 2004. **25**(17): p. 3707-3715.
5. Bhatia, S.N., et al., *Selective Adhesion of Hepatocytes on Patterned Surfaces.* Biochemical Engineering Viii, 1994. **745**: p. 187-209.
6. Hammarback, J.A., et al., *Guidance of Neurite Outgrowth by Pathways of Substratum-Adsorbed Laminin.* Journal of Neuroscience Research, 1985. **13**(1-2): p. 213-220.
7. Healy, K.E., B. Lom, and P.E. Hockberger, *Spatial-Distribution of Mammalian-Cells Dictated by Material Surface-Chemistry.* Biotechnology and Bioengineering, 1994. **43**(8): p. 792-800.
8. Charest, J.L., et al., *Polymer cell culture substrates with combined nanotopographical patterns and micropatterned chemical domains.* Journal of Vacuum Science & Technology B, 2005. **23**(6): p. 3011-3014.

9. Hu, W., et al., *Effects of nanoimprinted patterns in tissue-culture polystyrene on cell behavior.* Journal of Vacuum Science & Technology B, 2005. **23**(6): p. 2984-2989.

10. Zhu, B.S., et al., *Nanotopographical guidance of C6 glioma cell alignment and oriented growth.* Biomaterials, 2004. **25**(18): p. 4215-4223.

11. Peterbauer, T., et al., *Dynamics of the Alignment of Mammalian Cells on a Nano-Structured Polymer Surface.* Macromolecular Symposia, 2010. **296**(1): p. 272-277.

12. Peterbauer, T., et al., *Dynamics of Spreading and Alignment of Cells Cultured In Vitro on a Grooved Polymer Surface.* Journal of Nanomaterials, 2011. **2011**.

13. Wang, P.Y., H.T. Yu, and W.B. Tsai, *Modulation of Alignment and Differentiation of Skeletal Myoblasts by Submicron Ridges/Grooves Surface Structure.* Biotechnology and Bioengineering, 2010. **106**(2): p. 285-294.

14. Salber, J., et al., *Influence of different ECM mimetic peptide sequences embedded in a nonfouling environment on the specific adhesion of human-skin keratinocytes and fibroblasts on deformable substrates.* Small, 2007. **3**(6): p. 1023-1031.

15. De Silva, M.N., et al., *Two-step cell patterning on planar and complex curved surfaces by precision spraying of polymers.* Biotechnology and Bioengineering, 2006. **93**(5): p. 919-927.

16. Chaw, K.C., et al., *Matrigel coated polydimethylsiloxane based microfluidic devices for studying metastatic and non-metastatic cancer cell invasion and migration.* Biomedical Microdevices, 2007. **9**(4): p. 597-602.

17. Fu, G. and W.O. Soboyejo, *Cell/surface interactions of human osteo-sarcoma (HOS) cells and micro-patterned polydimelthylsiloxane (PDMS) surfaces.* Materials Science & Engineering C-Materials for Biological Applications, 2009. **29**(6): p. 2011-2018.

18. Lam, M.T., W.C. Clem, and S. Takayama, *Reversible on-demand cell alignment using reconfigurable microtopography.* Biomaterials, 2008. **29**(11): p. 1705-1712.

19. Choi, J.S., Y. Piao, and T.S. Seo, *Circumferential alignment of vascular smooth muscle cells in a circular microfluidic channel.* Biomaterials, 2014. **35**(1): p. 63-70.

20. Lee, A.A., et al., *Fluid shear stress-induced alignment of cultured vascular smooth muscle cells.* Journal of Biomechanical Engineering-Transactions of the Asme, 2002. **124**(1): p. 37-43.

21. Conway, D.E., et al., *Endothelial cell responses to atheroprone flow are driven by two separate flow components: low time-average shear stress and fluid flow reversal.* American Journal of Physiology-Heart and Circulatory Physiology, 2010. **298**(2): p. H367-H374.

22. Tzima, E., et al., *Activation of Rac1 by shear stress in endothelial cells mediates both cytoskeletal reorganization and effects on gene expression.* Embo Journal, 2002. **21**(24): p. 6791-6800.

23. Conway, D.E., et al., *Fluid Shear Stress on Endothelial Cells Modulates Mechanical Tension across VE-Cadherin and PECAM-1.* Current Biology, 2013. **23**(11): p. 1024-1030.

24. Malek, A.M. and S. Izumo, *Mechanism of endothelial cell shape change and cytoskeletal remodeling in response to fluid shear stress.* Journal of Cell Science, 1996. **109**: p. 713-726.

25. Shao, Y., et al., *Uniaxial cell stretching device for live-cell imaging of mechanosensitive cellular functions.* Review of Scientific Instruments, 2013. **84**(11).

26. Tremblay, D., et al., *A microscale anisotropic biaxial cell stretching device for applications in mechanobiology.* Biotechnology Letters, 2014. **36**(3): p. 657-665.

27. Shi, Y., et al., *Continuous Cyclic Mechanical Tension Inhibited Runx2 Expression in Mesenchymal Stem Cells Through RhoA-ERK1/2 Pathway.* Journal of Cellular Physiology, 2011. **226**(8): p. 2159-2169.

28. Koike, M., et al., *Effects of mechanical strain on proliferation and differentiation of bone marrow stromal cell line ST2.* Journal of Bone and Mineral Metabolism, 2005. **23**(3): p. 219-225.

29. Sumpio, B.E., et al., *Enhanced Collagen Production by Smooth-Muscle Cells during Repetitive Mechanical Stretching.* Archives of Surgery, 1988. **123**(10): p. 1233-1236.

30. Sumpio, B.E. and A.J. Banes, *Response of Porcine Aortic Smooth-Muscle Cells to Cyclic Tensional Deformation in Culture.* Journal of Surgical Research, 1988. **44**(6): p. 696-701.

31. Benes, A.J., et al., *A New Vacuum-Operated Stress-Providing Instrument That Applies Static or Variable Duration Cyclic Tension or Compression to Cells-Invitro.* Journal of Cell Science, 1985. **75**(Apr): p. 35-42.

32. Ignatius, A., et al., *Tissue engineering of bone: effects of mechanical strain on osteoblastic cells in type I collagen matrices.* Biomaterials, 2005. **26**(3): p. 311-318.

33. Wang, S.Q., et al., *Computational modeling of magnetic nanoparticle targeting to stent surface under high gradient field.* Computational Mechanics, 2014. **53**(3): p. 403-412.

34. Kreuter, J., *Nanoparticles as drug delivery systems for the brain.* Febs Journal, 2006. **273**: p. 35-35.

35. Sun, T.M., et al., *Engineered Nanoparticles for Drug Delivery in Cancer Therapy.* Angewandte Chemie-International Edition, 2014. **53**(46): p. 12320-12364.

36. Dreaden, E.C., et al., *Size matters: gold nanoparticles in targeted cancer drug delivery.* Therapeutic delivery, 2012. **3**(4): p. 457-478.

37. Park, J., et al., *Enhancement of surface ligand display on PLGA nanoparticles with amphiphilic ligand conjugates.* Journal of Controlled Release, 2011. **156**(1): p. 109-115.

38. Kettler, K., et al., *Cellular uptake of nanoparticles as determined by particle properties, experimental conditions, and cell type.* Environmental Toxicology and Chemistry, 2014. **33**(3): p. 481-492.

39. Huang, C.J., et al., *Substrate Stiffness Regulates Cellular Uptake of Nanoparticles.* Nano Letters, 2013. **13**(4): p. 1611-1615.

40. Lord, M.S., et al., *Cellular uptake and reactive oxygen species modulation of cerium oxide nanoparticles in human monocyte cell line U937.* Biomaterials, 2012. **33**(31): p. 7915-7924.

41. Rouse, J.G., et al., *Cyclic tensile strain increases interactions between human epidermal keratinocytes and quantum dot nanoparticles.* Toxicology in Vitro, 2008. **22**(2): p. 491-497.

42. Freese, C., et al., *In vitro investigation of silica nanoparticle uptake into human endothelial cells under physiological cyclic stretch.* Particle and Fibre Toxicology, 2014. **11**.

43. Hu, J., et al., *Enhanced Cell Adhesion and Alignment on Micro-Wavy Patterned Surfaces.* Plos One, 2014. **9**(8).

44. Feinberg, A.W., et al., *Systematic variation of microtopography, surface chemistry and elastic modulus and the state dependent effect on endothelial cell alignment.* Journal of Biomedical Materials Research Part A, 2008. **86A**(2): p. 522-534.

45. Su, W.T., Y.F. Liao, and I.M. Chu, *Observation of fibroblast motility on a micro-grooved hydrophobic elastomer substrate with different geometric characteristics.* Micron, 2007. **38**(3): p. 278-285.

46. He, R., et al., *Generation of Customizable Micro-wavy Pattern through Grayscale Direct Image Lithography.* Scientific Reports, 2016. **6**.

47. Wang, S.Q., Y. Wan, and Y.L. Liu, *Effects of nanopillar array diameter and spacing on cancer cell capture and cell behaviors.* Nanoscale, 2014. **6**(21): p. 12482-12489.

48. Harrison, R.G., *On the stereotropism of embryonic cells.* Science, 1911. **34**(0036-8075): p. 279-281.

49. Weiss, P., *In vitro experiments on the factors determining the course of the outgrowing nerve fiber.* Journal of Experimental Zoology, 1934. **68**(3): p. 393-448.

50. Curtis, A.S.G., and Malini Varde. "Control of cell behavior: topological factors." Journal of the National Cancer Institute 33.1 (1964): 15-26.

51. Doyle, A.D., Wang FW, Matsumoto K, Yamada KM (2009) One-dimensional topography underlies three-dimensional fibrillar cell migration. The Journal of cell biology, 184(4), 481-490.

52. James, C.D., Davis RC, Kam L, Craighead HG, Isaacson M, et al. (1998) Patterned protein layers on solid substrates by thin stamp microcontact printing. Langmuir, 14(4), 741-744.

53. Clark, P., Connolly P, Curtis AS, Dow JA, Wilkinson CD (1987) Topographical control of cell behaviour. I. Simple step cues. Development, 99(3), 439-448.

54. Wang, S.Q., et al., *Highly efficient and selective isolation of rare tumor cells using a microfluidic chip with wavy-herringbone micro-patterned surfaces.* Analyst, 2016. **141**(7): p. 2228-2237.

55. Shein, M., et al., *Engineered neuronal circuits shaped and interfaced with carbon nanotube microelectrode arrays.* Biomedical Microdevices, 2009. **11**(2): p. 495-501.

56. Lee, P.J., P.J. Hung, and L.P. Lee, *An artificial liver sinusoid with a microfluidic endothelial-like barrier for primary hepatocyte culture.* Biotechnology and Bioengineering, 2007. **97**(5): p. 1340-1346.

57. Nilsson, J., et al., *Review of cell and particle trapping in microfluidic systems.* Analytica Chimica Acta, 2009. **649**(2): p. 141-157.

58. Choudhury, D., et al., *Exploitation of physical and chemical constraints for three-dimensional microtissue construction in microfluidics.* Biomicrofluidics, 2011. **5**(2).

59. Kim, D.H., et al., *Nanoscale cues regulate the structure and function of macroscopic cardiac tissue constructs.* Proceedings of the National Academy of Sciences of the United States of America, 2010. **107**(2): p. 565-570.

60. Hsiao, A.Y., et al., *Microfluidic system for formation of PC-3 prostate cancer co-culture spheroids.* Biomaterials, 2009. **30**(16): p. 3020-3027.

61. Ho, C.T., et al., *Rapid heterogeneous liver-cell on-chip patterning via the enhanced field-induced dielectrophoresis trap.* Lab on a Chip, 2006. **6**(6): p. 724-734.

62. Anderson, D.E.J. and M.T. Hinds, *Endothelial Cell Micropatterning: Methods, Effects, and Applications.* Annals of Biomedical Engineering, 2011. **39**(9): p. 2329-2345.

63. Nielsen, D.H., *Fundamental Cardiovascular and Pulmonary Physiology - an Integrated Approach for Medicine - Green,Jf.* Physical Therapy, 1984. **64**(1): p. 126-126.

64. Pawlowski, K.J., et al., *Endothelial cell seeding of polymeric vascular grafts.* Frontiers in Bioscience-Landmark, 2004. **9**: p. 1412-1421.

65. Khare, K., J.H. Zhou, and S. Yang, *Tunable Open-Channel Microfluidics on Soft Poly(dimethylsiloxane) (PDMS) Substrates with Sinusoidal Grooves.* Langmuir, 2009. **25**(21): p. 12794-12799.

66. Lin, P. and S. Yang, *Spontaneous formation of one-dimensional ripples in transit to highly ordered two-dimensional herringbone structures through sequential and unequal biaxial mechanical stretching.* Appl. Phys. Lett., 2007. **90**(24): p. 241903.

67. Bowden, N., et al., *The controlled formation of ordered, sinusoidal structures by plasma oxidation of an elastomeric polymer.* Appl. Phys. Lett., 1999. **75**(17): p. 2557-2559.

68. Stafford, C.M., et al., *A buckling-based metrology for measuring the elastic moduli of polymeric thin films.* Nat. Mater., 2004. **3**(8): p. 545-550.

69. Yang, J.-T., K.-J. Huang, and Y.-C. Lin, *Geometric effects on fluid mixing in passive grooved micromixers.* Lab on a Chip, 2005. **5**(10): p. 1140-1147.

70. Yuen, P.K. and V.N. Goral, *Low-cost rapid prototyping of flexible microfluidic devices using a desktop digital craft cutter.* Lab on a Chip, 2010. **10**(3): p. 384-387.

71. Wan, Y., et al., *Nanotextured substrates with immobilized aptamers for cancer cell isolation and cytology.* Cancer, 2012. **118**(4): p. 1145-1154.

72. Satyanarayana, S., R.N. Karnik, and A. Majumdar, *Stamp-and-stick room-temperature bonding technique for microdevices.* Journal of Microelectromechanical Systems, 2005. **14**(2): p. 392-399.

73. Eddings, M.A., M.A. Johnson, and B.K. Gale, *Determining the optimal PDMS-PDMS bonding technique for microfluidic devices.* Journal of Micromechanics and Microengineering, 2008. **18**(6): p. -.

74. Young, E.W.K., A.R. Wheeler, and C.A. Simmons, *Matrix-dependent adhesion of vascular and valvular endothelial cells in microfluidic channels.* Lab on a Chip, 2007. **7**(12): p. 1759-1766.

75. Vankooten, T.G., et al., *Influence of Substratum Wettability on the Strength of Adhesion of Human Fibroblasts.* Biomaterials, 1992. **13**(13): p. 897-904.

76. Yang, J., et al., *Plasma-treated, collagen-anchored polylactone: Its cell affinity evaluation under shear or shear-free conditions.* Journal of Biomedical Materials Research Part A, 2003. **67A**(4): p. 1139-1147.

77. Patrizia Nigro, J.-i.A., and Bradford C. Berk., *Flow Shear Stress and Atherosclerosis: A Matter of Site Specificity.* Antioxidants & Redox Signaling, 2011. **15**(5): p. 1405-1414.

78. Lheureux, N., et al., *Invitro Construction of a Human Blood-Vessel from Cultured Vascular Cells - a Morphologic Study.* Journal of Vascular Surgery, 1993. **17**(3): p. 499-509.

79. Vunjak-Novakovic, G., et al., *Dynamic cell seeding of polymer scaffolds for cartilage tissue engineering.* Biotechnology Progress, 1998. **14**(2): p. 193-202.

80. Hakkinen, K.M., et al., *Direct Comparisons of the Morphology, Migration, Cell Adhesions, and Actin Cytoskeleton of Fibroblasts in Four Different Three-Dimensional Extracellular Matrices.* Tissue Engineering Part A, 2011. **17**(5-6): p. 713-724.

81. Wozniak, M.A., et al., *Focal adhesion regulation of cell behavior.* Biochimica Et Biophysica Acta-Molecular Cell Research, 2004. **1692**(2-3): p. 103-119.

82. Baumann, K., *Cell Migration Moving in 3d.* Nature Reviews Molecular Cell Biology, 2010. **11**(7): p. 465-465.

83. Baker, B.M. and C.S. Chen, *Deconstructing the third dimension - how 3D culture microenvironments alter cellular cues.* Journal of Cell Science, 2012. **125**(13): p. 3015-3024.

84. Andreescu, S., *Nanoparticle-based technologies for diagnosis and therapy.* Abstracts of Papers of the American Chemical Society, 2012. **244**.

85. Jiang, L.Q., et al., *Cellular uptake mechanism and intracellular fate of hydrophobically modified pullulan nanoparticles.* International Journal of Nanomedicine, 2013. **8**: p. 1825-1834.

86. Xu, A.R., et al., *A physical model for the size-dependent cellular uptake of nanoparticles modified with cationic surfactants.* International Journal of Nanomedicine, 2012. **7**: p. 3547-3554.

87. Huang, X.L., et al., *The effect of the shape of mesoporous silica nanoparticles on cellular uptake and cell function.* Biomaterials, 2010. **31**(3): p. 438-448.

88. Nam, H.Y., et al., *Cellular uptake mechanism and intracellular fate of hydrophobically modified glycol chitosan nanoparticles.* Journal of Controlled Release, 2009. **135**(3): p. 259-267.

89. Zetter, B.R., *The Endothelial-Cells of Large and Small Blood-Vessels.* Diabetes, 1981. **30**: p. 24-28.

90. De Jong, W.H. and P.J.A. Borm, *Drug delivery and nanoparticles: Applications and hazards.* International Journal of Nanomedicine, 2008. **3**(2): p. 133-149.

91. Zhang, L.W. and N.A. Monteiro-Riviere, *Mechanisms of Quantum Dot Nanoparticle Cellular Uptake.* Toxicological Sciences, 2009. **110**(1): p. 138-155.

92. Mailander, V., et al., *Carboxylated superparamagnetic iron oxide particles label cells intracellularly without transfection agents.* Molecular Imaging and Biology, 2008. **10**(3): p. 138-146.

93. Dausend, J., et al., *Uptake Mechanism of Oppositely Charged Fluorescent Nanoparticles in HeLa Cells.* Macromolecular Bioscience, 2008. **8**(12): p. 1135-1143.

94. Azuma, N., et al., *Endothelial cell response to different mechanical forces.* Journal of Vascular Surgery, 2000. **32**(4): p. 789-794.

95. Chapman, G.B., et al., *Physiological cyclic stretch causes cell cycle arrest in cultured vascular smooth muscle cells.* American Journal of Physiology-Heart and Circulatory Physiology, 2000. **278**(3): p. H748-H754.

96. Morioka, M., et al., *Microtubule Dynamics Regulate Cyclic Stretch-Induced Cell Alignment in Human Airway Smooth Muscle Cells.* Plos One, 2011. **6**(10).

97. Birukov, K.G., *Cyclic Stretch, Reactive Oxygen Species, and Vascular Remodeling.* Antioxidants & Redox Signaling, 2009. **11**(7): p. 1651-1667.

98. Eldib, M. and D.A. Dean, *Cyclic Stretch of Alveolar Epithelial Cells Alters Cytoskeletal Micromechanics.* Biotechnology and Bioengineering, 2011. **108**(2): p. 446-453.

99. Sharei, A., et al., *Plasma membrane recovery kinetics of a microfluidic intracellular delivery platform.* Integrative Biology, 2014. **6**(4): p. 470-475.

100. Hatami, J., et al., *Influence of Cyclic Stretch on Mechanical Properties of Endothelial Cells.* Experimental Mechanics, 2013. **53**(8): p. 1291-1298.

101. Sweeney, N.V., et al., *Cyclic strain-mediated regulation of endothelial matrix metalloproteinase-2 expression and activity.* Cardiovascular Research, 2004. **63**(4): p. 625-634.

102. Colombo, A., P.A. Cahill, and C. Lally, *An analysis of the strain field in biaxial Flexcell membranes for different waveforms and frequencies.* Proceedings of the Institution of Mechanical Engineers Part H-Journal of Engineering in Medicine, 2008. **222**(H8): p. 1235-1245.

103. Win, K.Y. and S.S. Feng, *Effects of particle size and surface coating on cellular uptake of polymeric nanoparticles for oral delivery of anticancer drugs.* Biomaterials, 2005. **26**(15): p. 2713-2722.

104. Huh, D., et al., *Reconstituting Organ-Level Lung Functions on a Chip.* Science, 2010. **328**(5986): p. 1662-1668.

105. Groneberg, D.A., et al., *Nanoparticle-based diagnosis and therapy.* Current Drug Targets, 2006. **7**(6): p. 643-648.

106. Davidovich, N., et al., *Cyclic Stretch-Induced Oxidative Stress Increases Pulmonary Alveolar Epithelial Permeability.* American Journal of Respiratory Cell and Molecular Biology, 2013. **49**(1): p. 156-164.

107. Gervasio, O.L., et al., *Caveolae respond to cell stretch and contribute to stretch-induced signaling.* Journal of Cell Science, 2011. **124**(21): p. 3581-3590.

108. Kiyoshima, D., et al., *Force-and Ca2+-dependent internalization of integrins in cultured endothelial cells.* Journal of Cell Science, 2011. **124**(22): p. 3859-3870.

109. Dai, J. and M.P. Sheetz, *Regulation of endocytosis, exocytosis, and shape by membrane tension.* Cold Spring Harbor Symposia on Quantitative Biology, 1995. **60**: p. 567-571.

110. Chang, S., et al., *Phenotypic modulation of primary vascular smooth muscle cells by short-term culture on micropatterned substrate.* PLoS One, 2014. **9**(2): p. e88089.

111. Qaddoumi, M.G., et al., *The characteristics and mechanisms of uptake of PLGA nanoparticles in rabbit conjunctival epithelial cell layers.* Pharmaceutical Research, 2004. **21**(4): p. 641-648.

112. Samuel, S.P., et al., *Multifactorial determinants that govern nanoparticle uptake by human endothelial cells under flow.* International Journal of Nanomedicine, 2012. **7**: p. 2943-2956.

113. Hu, J. and Y.L. Liu, *Cyclic Strain Enhances Cellular Uptake of Nanoparticles.* Journal of Nanomaterials, 2015.

VITA

Jia Hu is a Ph. D. student of Dr. Yaling Liu at Lehigh University. She was born in Sichuan, China. She received her Bachelor of Engineer degree in Bioengineering from Chongqing University in 2011. Her research interest is in biomechanics and microfluidics. Her main research topics include cellular uptake of nanoparticles under cyclic stretch, cell adhesion on micro-patterned substrates and DNA nanoparticle molecular strain sensor.

EDUCATION

Ph.D.,**Lehigh University**, Bethlehem, PA May 2016

Mechanical Engineering and Mechanics

B.S.,**Chongqing University**, ChinaJun 2011

Bioengineering and Biomedical Engineering

PROFESSIONAL SKILLS

Specialty	Cell Culture, Cell-based Assay, Surface Chemistry Functionalization, Immunofluorescence Assay, Fluorescent Imaging, Nanotechnology
Processing	PCR, Gel Electrophoresis, HPLC, DNA Isolation, Protein Isolation, Chromatography, Photolithography, PDMS, Sonication, Sterilization, Western Blot
Fabrication	Microfluidic Device Fabrication in Clean Room, DNA Nano/micro-particle Structure Assembly
Characterization	SEM, UV-Vis Spectrometry, Confocal Microscopy, Flow Cytometry, Microplate Reader, Fluorescence Microscopy, Particle Size Measurement
Computer Skills	MatLab, Python, SolidWorks, Image J, AutoCAD, Microsoft Office